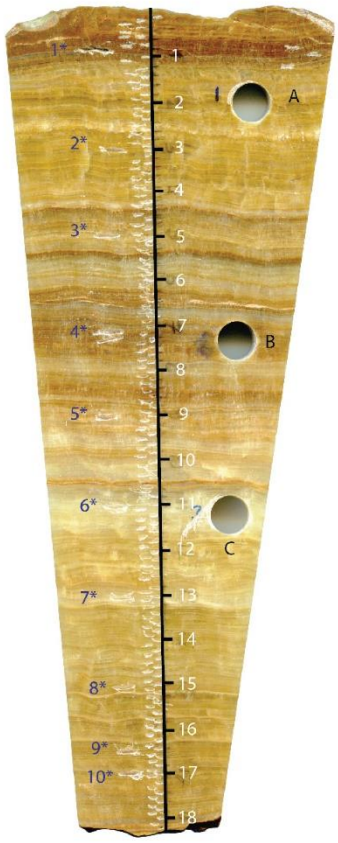

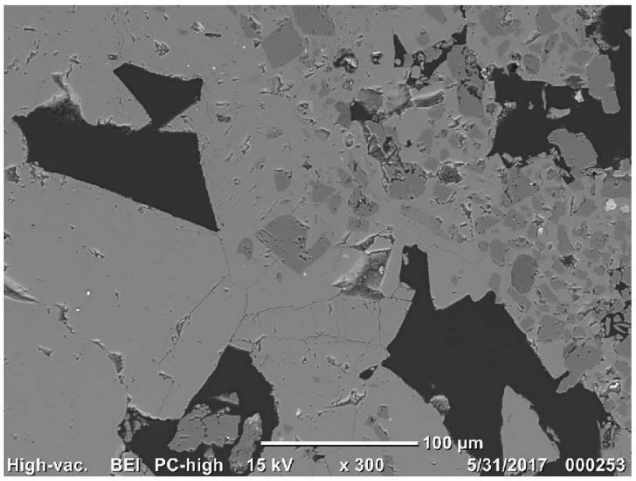

Climate reconstruction of southern France based on a speleothem from Montagne Noire

BSc project VU Amsterdam
Course code: AB_1096

F.R. van Bakel
2555059

22-07-2017

Supervisors:
Dr. M. Sánchez-Román
(m.sanchezroman@vu.nl)

Dr. H.J.L. van der Lubbe
(h.j.l.vander.lubbe@vu.nl)

VU VRIJE UNIVERSITEIT AMSTERDAM
Faculty of Earth and Life Sciences

Abstract

Montagne Noire, part of the southern Massif Central in France, is the border between two climate types and therefore, it has always been subject to major and minor changes in temperature, rainfall and vegetation. This study aims to reconstruct the local paleoclimate of southern France by using a multi-proxy approach based on mineralogical (X-ray diffraction), geochemical (stable isotopes: C, O, H) and microscopic (scanning electron, petrographic and colour) analyses in a speleothem from Mélagues, located on the northern side of Montagne Noire.

Temperature, rainfall and vegetation changes over time in the Mélagues region have been studied using the stable isotopic composition recorded in the speleothem. Although no dating of this speleothem is available yet, this study also examined possible relations with other regions and climate oscillations.

Microscopic analyses of thin sections together with XRD analyses allowed us to determine the morphology, texture and mineralogy of the speleothem, which is composed of a mixture of magnesium calcite (~70%), dolomite (~25%, possibly formed through diagenetic processes) and a very low content of quartz (~5%). Partial dissolution (~5%) of the speleothem led to small voids (<40 µm) that were subsequently (partially) refilled by bacteria and microorganisms. Four columnar fabrics (compact, open, elongated and spherulitic) are observable in the studied speleothem, along with micrite, microsparite and mosaic fabrics. All these fabrics reflect (post-)depositional and environmental changes.

The average temperature (~14.8 °C) and vegetation (C3 plants) during deposition resemble the present-day temperature (14.8 ± 0.9 °C) and vegetation around our study site. Relatively high average $\delta^{18}O$ values (-4.38‰, 1σ ≈ 0.37) and relatively low average $\delta^{13}C$ values (-9.36‰, 1σ ≈ 0.55) of the stalagmite led us to interpret that the stalagmite was mainly deposited in a relatively warm and dry period, while seasonal precipitation from the Mediterranean Sea dominates the record. A deposition of speleothems in a relatively dry climate is exceptional, but also low water yields (<0.1 µl) in fluid inclusions support this interpretation. Therefore, this study provides important new insights in the formation of speleothems in this region.

Although the precise controls on the relation between visual colours and geochemical composition in speleothems are poorly understood, it is reasonable to assume reddish-brown and colourless layers in the speleothem formed during relatively wet and dry periods, respectively. Small-scale periodicities (<5 mm) of carbon and oxygen isotopes in the Montagne Noire record probably reflect (multi)decadal oscillations and the single larger cycle (±120 mm) could also reflect multi-centennial up to millennial time-scale oscillations. A Holocene stalagmite from Scladina (Belgium) and modern active calcite deposits in the Clamouse Cave (France) show similar oxygen and carbon isotope values, which might reflect resemblances in environmental conditions during deposition. Nevertheless, dating of the studied speleothem needs to be performed to confirm hypotheses regarding comparisons with other regions and climate oscillations.

Contents

1. Introduction

1.1. Introductory remarks about speleothems

Speleothems are excellent recorders of past regional climatic and environmental conditions. These crystalline cave deposits of calcium carbonate ($CaCO_3$) occur in many forms, such as stalagmites (which grow upward from the floor of caves beneath a drip site), stalactites (growing downward from the roof of a cave) and flowstones (sheet-like horizontally or inclined layers of calcite spread as a film across a cave floor or wall; Schwarcz, 2007). Speleothems have the potential to be as influential as ice cores have been in the past: "*For paleoclimate, the past two decades have been the age of the ice core. The next two may be the age of the speleothem*" (Henderson, 2006). Speleothems even have several advantages in comparison to other climate archives like ice cores, tree rings, ocean and lake sediments (Fleitmann and Spötl, 2008), since speleothems

(1) have a global distribution;
(2) can be dated with extremely high precision (up to around 600 kyr BP) using the absolute U/Th-dating techniques, potentially making climatic periodicities and events clearly visible;
(3) can grow constantly over long time intervals (up to around 100.000 years), while maintaining the high-resolution recording of climatic conditions.

Speleothems therefore provide long high-resolution records that can be interpreted as changes in conditions of deposition in the karstic cave and thus reflecting the Earth's surface processes above. Proxies that have been successfully derived from speleothems include oxygen isotopic composition ($\delta^{18}O$), carbon isotopic composition ($\delta^{13}C$), trace element concentrations (e.g., Sr, Ba, U), isotopic compositions of fluid inclusions (seepage water trapped during growth), as well as growth rate/annual band thickness (Partin et al., 2008; Schwarcz, 2007).

1.2. Research aims & study site

Nowadays, Montagne Noire in southern France is at the border between two climate types: an oceanic-influenced climate on the (north)west side of the mountains and a Mediterranean-influenced climate in the (south)east (Inventaire Forestier National, 1989; Inventaire Forestier National, 1995). Therefore, this area is key to study climate change. To understand climate change at a broader scale and changes in precipitation in particular, a dense network of paleo-rainfall records is necessary. A low amount of speleothem records in southern France strengthens the reason why a study in this area should be performed. This research is done in the context of the 3rd years BSc Earth Sciences at the Vrije Universiteit in Amsterdam. The main aim is to reconstruct the (local) paleoclimate of southern France by measuring carbon ($^{13/12}C$), oxygen ($^{18/16}O$) and hydrogen ($^{2/1}H$) isotope values of a speleothem from Montagne Noire (southern Massif Central). The link between our results and other regional/paleoclimate proxy records as well as global climate changes is also investigated. Lastly, the composition of the speleothem aids in understanding the environmental conditions during and after its formation.

In order to answer the main research question "*How did the paleoclimate around Montagne Noire (southern France) develop during the forming of the speleothem and how does this relate to other regions and climate oscillations?*" the following sub-questions have been posed:

- How did oxygen, hydrogen and carbon isotope compositions and visual appearance change over time?
- How did the temperature, rainfall and vegetation change over time?
- How can these results be linked to natural variabilities and climate oscillations on different scales (e.g., Dansgaard-Oeschger cycles, Milankovitch cycles, North Atlantic Oscillation, summer insolation)?
- What is the speleothem composed of?

Mineralogical (X-ray diffraction), geochemical (stable isotopes) and microscopic (scanning electron, petrographic and colour) analyses are used to answer these questions (2. Methodology). The age of the speleothem is not well-constrained yet. However, it has possibly formed during an interglacial in the Quaternary period, since speleothems mainly form in wet and warm conditions and often do not grow during glacials. However, the age and/or time span of this speleothem might be estimated by comparing its geochemical data to other records.

The speleothem was taken from a karstic cavity encased in lower Cambrian dolostones crosscut by the road D-52 in Montagne Noire (43°44'32.96'' N, 03°00'50.31'' E), 2 km to the NW of Mélagues (Aveyron, Midi-Pyrénées, Occitanie, France; Fig. 1.1).

Figure 1.1. The geographical location of the study area in France (upper image). Zoomed in satellite view of the study area and its surroundings (lower image). The exact location of the crosscut is marked by a yellow star, while the red box in the upper image displays the extent of the area in the lower image. Modified after Google Maps (2017a); Google Maps (2017b).

The Mélagues paleokarst developed in impure arranged monoclinal structures dipping to the north. The present-day disposition of the karstic bedding is subhorizontal, while the section made by the road is elliptical in outline. Besides that, the section displays multiphase features with a sequence of events reflecting dissolution by meteoric waters and filling of void spaces by speleothems, a mosaic of calcite cements and breccia levels (Fig. 1.2).

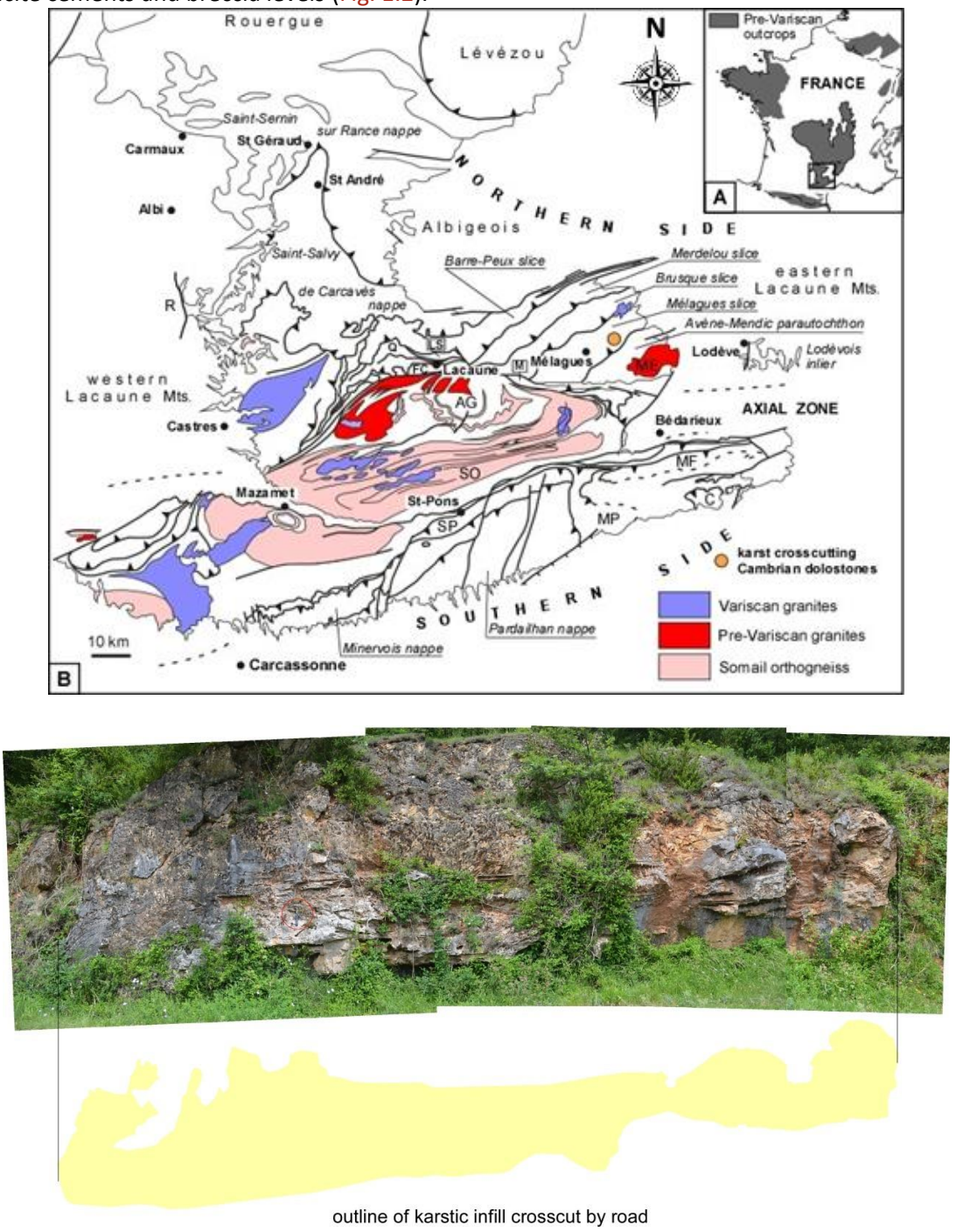

Figure 1.2. Large-scale geological setting (above, location in orange; modified after Álvaro et al. (2014)) and crosscut of the study area: an exposure of the lower Cambrian Lastours Formation exhibiting a complex karstic cavity infilled with speleothems (below) close to Mélagues, northern Montagne Noire, France.

1.3. Geological setting

Montagne Noire is the southern prolongation of the French Massif Central and a segment of the external regions of the southwestern European Variscan Belt. Folded and thrust rocks of the French Massif Central are exposed in the northern Montagne Noire and form a continuous highland chain (Álvaro et al., 2014). The Montagne Noire appears as a complex antiform of numerous tectonic units, which have been grouped into three ENE-WSW-trending macrostructural domains (Fig. 1.3): a metamorphic Axial Zone containing Variscan eclogites bounded by the other two domains on its southern and northern flanks (Álvaro et al., 2014).

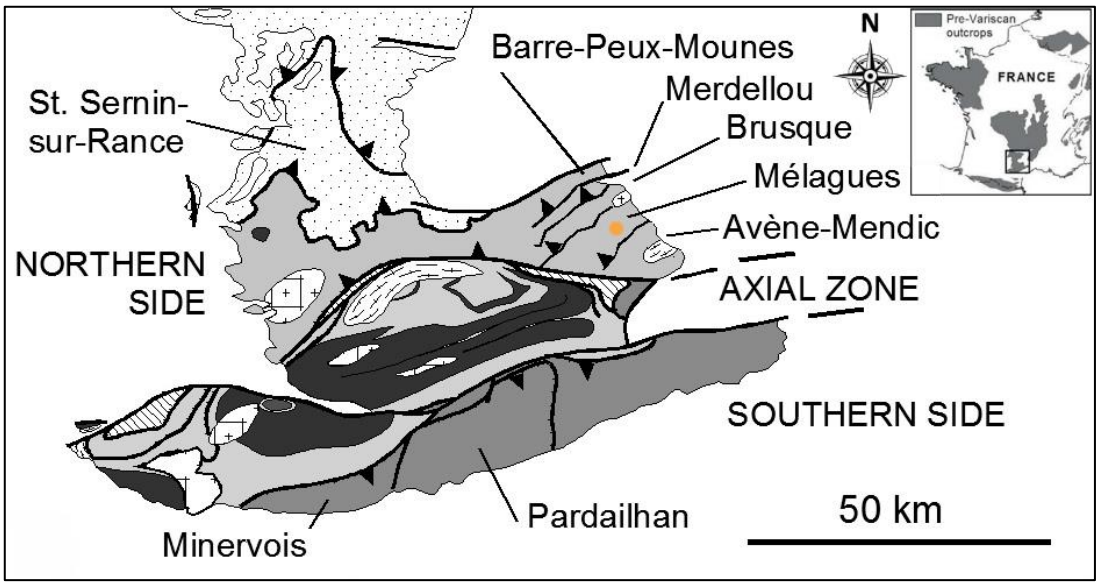

Figure 1.3. Macrostructural domains of Montagne Noire and its slices (grey), with in orange the location of the study site. Modified after Álvaro et al. (2010).

As can be inferred from figures 1.2 & 1.3, the study site is part of the Mélagues slice on the northern side of Montagne Noire, accompanied by the Avène-Mendic (southeast) and Brusque (northwest) slices. The lower Cambrian part of this slice mainly consist of the Marcory, Pardailhan and Lastours Formations (Fig. 1.4; Álvaro et al., 2014). These formations may differ little on both sides of Montagne Noire, but for this research only the Lastours Formation on the northern side was taken into consideration, since the karstic cavity is encased there.

Lastours Formation

The Lastours Formation of the Mélagues slice is a monotonous, hardly weathering carbonate unit, which is 200-400 m thick and exposed at the top of many hills and creeks. The Lastours Formation is dominated by yellowish, massive to bedded dolostones with a common facies-destructive replacement of calcite. Its fossil content consists of some archaeocyathan debris (*Coscinocyathus*) and the trilobite *Micmacca albesensis*. Exposures of the formation in the southern Montagne Noire mainly consist of stacked microbial-archaeocyathan reefs and bedded carbonates locally containing trilobites and skeletonized microfossils of Cambrian Epoch 2 age (Álvaro et al., 1998a; Álvaro et al., 1998b; Álvaro et al., 2000; Álvaro et al., 2002; Álvaro et al., 2010).

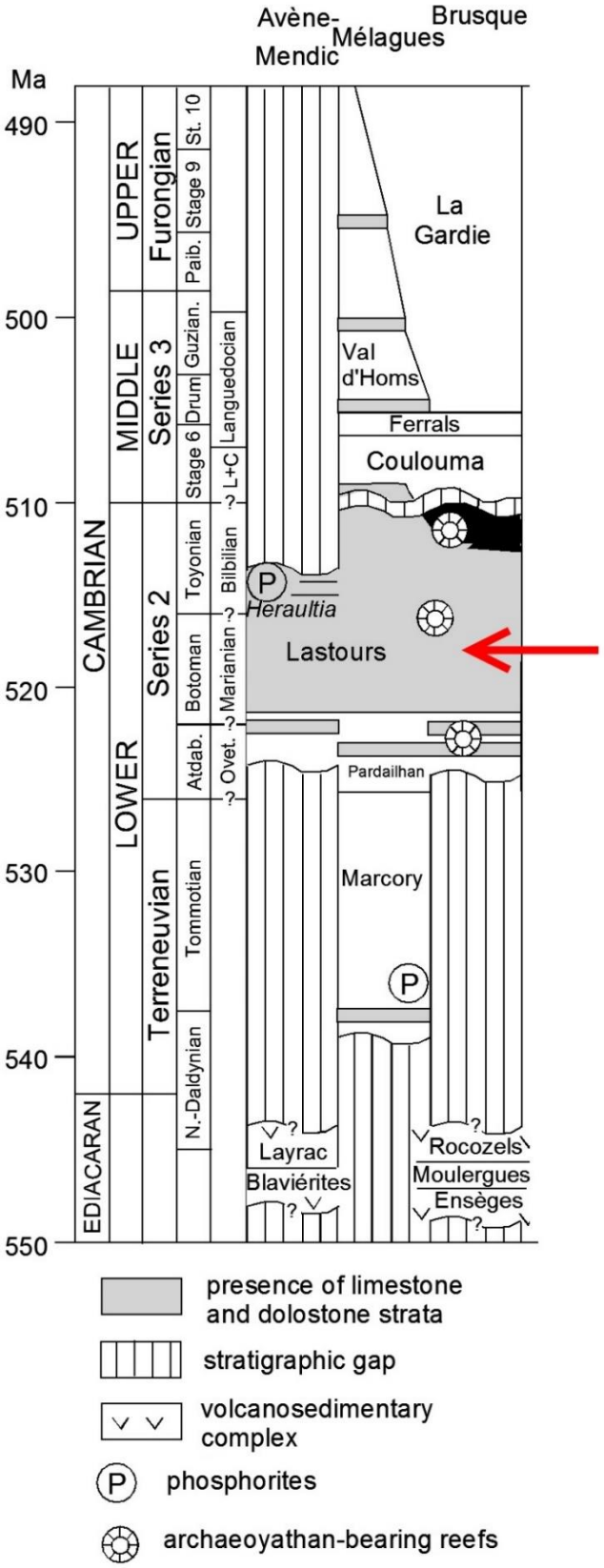

Figure 1.4. Stratigraphic column of Montagne Noire, specified for the Mélagues and its surrounding slices. The Lastours Formation is indicated with a red arrow. Modified after Álvaro et al. (2010).

1.4. Present-day climate

As aforementioned, Montagne Noire nowadays is the border between two climate types: an oceanic-influenced climate on the (north)western side of the mountains and a Mediterranean-influenced climate in the (south)east, or Cfb (temperate climate with a warm summer, but without a dry season) and Csa (temperate climate with a dry and hot summer), respectively, according to the Köppen climate classification (Inventaire Forestier National, 1989; Inventaire Forestier National, 1995). As can be inferred from figure 1.5, summers are slightly drier than other seasons, while the average temperature remains between approximately 5 and 20 degrees Celsius. The 11-year (2003-2013) annual mean temperature in Avignon, about 150 km east of Mélagues, shows the most representative measurements in the region and is 14.8 ± 0.9 °C. (Comité départemental du tourisme de l'Aude, 2012; IAEA/WMO, 2013; Inventaire Forestier National, 1995; Inventaire Forestier National, 1989). Average modern isotope values of rainfall and calcite deposits are presented in table 1.1.

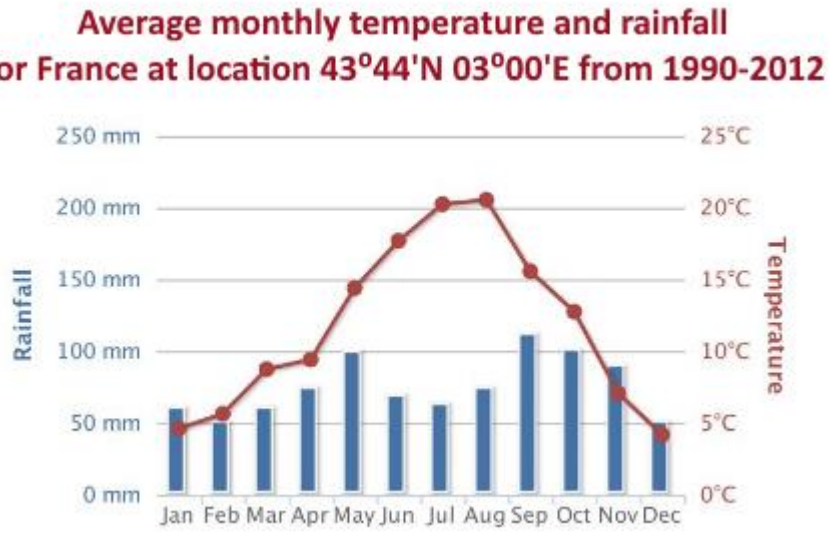

Figure 1.5. Average monthly temperature and rainfall for France at coordinates 43°44'N 03°00'E from 1990-2012 (The World Bank Group, n.d.).

Isotope	Value (‰)
$\delta^{13}C_{calcite}$	-7.4 to -9.6
$\delta^{18}O_{calcite}$	-4.3 to -5.5
$\delta^{18}O_{rain}$	-5.7 ± 1.1
$\delta^{2}H_{rain}$	-38.1 ± 7.9

Table 1.1. Overview of stable isotopes in present-day rainfall and calcite deposits. Calcite data is from the Clamouse Cave, relative to VPDB (Plagnes et al., 2002) and average annual rainfall data from Avignon, relative to V-SMOW (IAEA/WMO, 2013).

Oceanic winds from west to southwest are dominant (Inventaire Forestier National, 1995). Montagne Noire obstructs these large masses of humid, warm air coming from the Atlantic Ocean, while colder northern winds mainly blow during winter, both leading to approximately 1000 to 1500 mm precipitation per year in and around our study site. However, precipitation at the Clamouse Cave site (45 km east of our study site) has a Mediterranean origin in summer (violent storms) and fall, while during spring, precipitation is due to the interaction of air masses from both Atlantic and Mediterranean origin (Plagnes et al., 2002). Part of this precipitation falls as snow, which can cover the ground for up to two months (Inventaire Forestier National, 1995; Salomon and Bou, 2012). As a result, infiltration of water and the release of organic acids by the abundant (forest) vegetation can easily lead to the karst phenomena, which can be found on Montagne Noire, especially at higher altitudes.

The study site is located at about 680 m altitude in a valley, surrounded by mountains ranging between 800 and 860 m in altitude. On a larger scale, altitude increases towards the SW and decreases

in NW and SE directions. Runoff at our study site is transported to the Atlantic Ocean via Le Thalis, adjacent to the road at our study site, La Nuéjouls, Le Dourdou de Camarès, Le Tarn and in the end La Garonne (Google Maps, 2017c). The area covered by forests in the region is remarkably high in the region of our study site: 57,3%. The hills are usually wooded with beech and mostly mixed with oak, while about a third of the forest vegetation consists of coniferous trees. The moors and pastures are extensive, but a large part has been reforested (Inventaire Forestier National, 1995). The presence of beech trees indicates underlying soils are mostly acidic, calcareous, moist and well-drained (Caroll, 2015).

1.5. Previous paleoclimate research around southern France

As aforementioned, not much paleoclimate or speleothem research has been performed in the region of Montagne Noire, which makes this thesis a pioneering one.

Speleothems in Grotte de Clamouse (Saint-Jean-de-Fos, Hérault), about 45 km east of Mélagues, have been investigated by multiple scientists throughout the last decades, but this cave is not considered to be part of Montagne Noire. Fairchild et al. (2000) found four controlling processes on Mg/Ca and Sr/Ca concentrations, Frisia et al. (2002) studied the formation and habits of aragonite, McDermott et al. (1999) concluded that $\delta^{18}O$ and stalagmite extension rates are correlated, suggesting that temperature may have been an important first-order control on $\delta^{18}O$ variations at this site. McMillan et al. (2005) found a multi-decadal period of aridity (1200–1100 yr BP), based on trace element compositions. Additionally, Plagnes et al. (2002) showed that a speleothem in the cave grew discontinuously during warm and humid phases (MIS 5.1, 5.3, 5. 5 and 7), as well as during a brief period during the glacial stage MIS 6.

Another karstic cave in France, which has been studied to a lesser extent by paleoclimatologists, is Grotte de Villars (Villars, Dordogne), located about 260 km northwest of Mélagues. A study from Genty et al. (2003) reveals rapid climate oscillations coincide with established Dansgaard–Oeschger events between 83,000 and 32,000 years ago using carbon and oxygen isotope records and also provides evidence for a long phase of extremely cold climate in southwest France between 61.2 ± 0.6 and 67.4 ± 0.9 kyr ago. A study of Genty et al. (2010) extensively investigated rapid climate events, which are correlated with Atlantic and Mediterranean pollen records.

Other paleoclimate or speleothem research in southern France has been established from south-east France to south-east Spain by Jalut et al. (2000), in Grotte des Perles (about 5 km southwest of Mélagues) by Salomon and Bou (2012) and in the northwestern parts of the Iberian Peninsula by Stoll et al. (2013). The first mentioned study identified six major changes in vegetation cover by using pollen ratios, while the second study described the presence of speleothems in Montagne Noire. The latter authors successfully evaluated if there are patterns in stalagmite growth that are evidence of climatic forcing. A final research in the Pont-de-Ratz Cave, 35 km southeast of Mélagues, identified the original and diagenetic features in aragonite-calcite speleothems (Perrin et al., 2014).

1.6. Structure of thesis

Hereafter, additional background information will be provided about speleothems in general. In the next chapter, the methodology will be elaborated on, in which the used methods and theoretical background will be explained. The results of this investigation will be presented in chapter 3, using the lab data. In chapter 4 and 5, respectively the discussion and conclusion will be presented. At first, the results will be interpreted and linked to previous research mentioned above and subsequently the answers to the research questions will be discussed. Finally, future recommendations are given in chapter 6, followed by acknowledgements and references.

The appendices consist of the figure captions (Appendix I), lab data tables (Appendix II), graphs (Appendix III), speleothem images (Appendix IV), SEM & EDS results (Appendix V) and XRD data (Appendix VI).

1.7. Speleothem background information

To gain a better understanding of what the results represent, it is necessary to elaborate on the current knowledge of the formation of speleothems.

Before percolating through the bedrock, surface water is first exposed to atmospheric CO_2 and then to soil gases enriched in biogenic CO_2 (Fig. 1.6). Depending on the nature of the openings, which it passes, the percolating water can react extensively with the rock or may pass through with relatively little chemical interaction. Under conditions of diffuse flow through relatively tight fractures and joints, the water can approach chemical and isotopic equilibrium with the rock, whereas in larger, open channels entering caves, surface water may enter essentially unchanged (Schwarcz, 2007). As soon as the water enters the cave, drip waters can start to precipitate calcium carbonate ($CaCO_3$) as a result of two processes: (1) evaporation, which increases the concentration of calcium ions until the solubility of $CaCO_3$ is exceeded, and (2) outgassing of CO_2 from the water, which results in the slow precipitation of calcium carbonate: $Ca^{2+} + 2\ HCO_3^- \rightarrow CaCO_3 + H_2O + CO_2$. The calcium carbonate potentially contains a number of distinct isotopic signals, recorded as variations in the relative abundance of the isotopes of Ca, O and C (Schwarcz, 2007).

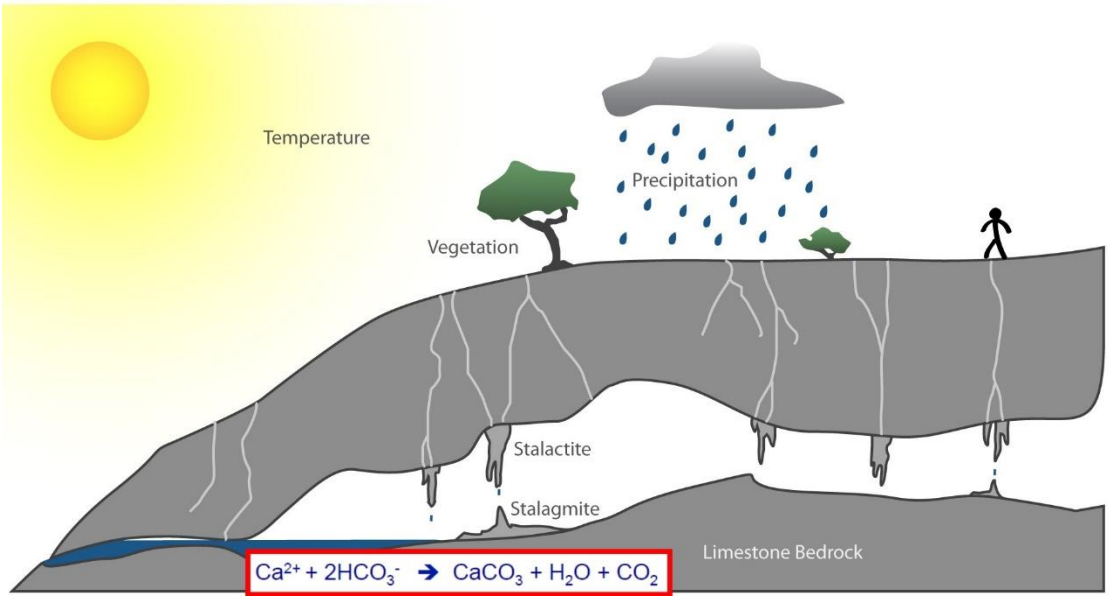

Figure 1.6. Schematic representation of how speleothems are formed and influenced. Modified after Fairchild (2013).

1.7.1. Carbon isotopes

The $\delta^{13}C$ values in speleothem calcite directly reflect the isotopic composition of the drip water from which the speleothem grew, because the temperature dependence of the carbon isotopic fractionation between calcite and dissolved inorganic carbon (DIC) is relatively small (Schwarcz, 2007). Carbon taken up by the percolating water will reflect the bedrock composition in a closed system (limestone), atmospheric CO_2, type of surface vegetation, cave conditions during dissolution (open/closed) and organic components in the soils (details below; McDermott, 2004; Schwarcz, 2007; Van Breukelen, 2009). These factors may in part be linked to humidity and in turn rainfall. Within the lower epikarst and cave itself, seasonal hydrological and/or ventilation factors and longer-term dry conditions can cause a variable shift to heavier carbon isotope values (Fairchild et al., 2006).

Although separating the different sources of carbon is challenging, all effects are (potentially) influenced by climate changes like amount of precipitation and temperature (Van Breukelen, 2009). Variations in $\delta^{13}C_{ct}$ (the $\delta^{13}C$ value of calcite) are mainly caused by two effects:

- Change in the proportion of C3 to C4 plants, which have different types of carbon fixation in photosynthesis, growing above the cave: $\delta^{13}C$ values of C4 plants are 17‰ higher than those of C3 plants. Most C4 plants are grasses, so shifts from forest to grassland can cause an increase in $\delta^{13}C$ in speleothem calcite and vice versa.
- Change in the density of vegetation above the cave: dissolution of limestone in the absence of soil cover occurs by reaction with atmospheric CO_2, leading to higher $\delta^{13}C$ values of DIC in recharge water compared to that produced under C3- and C4-based soils (Schwarcz, 2007).

In addition, conditions of dissolution have an important bearing on the $\delta^{13}C$ of cave water and hence that of the speleothem calcite. A study by (McDermott, 2004) defined two end-member models, which describe the processes by which percolating groundwaters acquire calcium carbonate in the soil and in host rocks above the cave. The first model is an open-system model, where continuous equilibration occurs between the seepage water and an infinite reservoir of soil CO_2. This process drives a monotonic increase in bicarbonate content as the water progressively acquires more solutes in the unsaturated zone. Under these conditions the $\delta^{13}C$ composition of the dissolved species reflects the *isotopic composition of the soil CO_2*, with no detectable isotopic imprint from the carbonate host-rock. In the second model, a closed system-model, the percolating water becomes isolated from the soil CO_2 reservoir as soon as carbonate dissolution commences, which is limited by the finite CO_2 reservoir. Under these closed system conditions the *isotopic composition of the carbonate host-rock influences the isotopic composition of the DIC*. This results in isotopically lighter precipitates in the open system and heavier ones in a closed system. In practice, most natural systems are likely to be partially open.

Several studies have found correlated shifts in $\delta^{18}O$ and $\delta^{13}C$ in the calcite of speleothems reflecting coupled changes in vegetation and temperatures, whereas other studies show distinctly independent trends for each isotopic signal (Schwarcz, 2007). Thus, values of $\delta^{13}C$ isotopes may give some indication of past climate changes, but precise interpretation remains difficult, since there are many different carbon reservoirs which all interact with each other.

As aforementioned, large shifts in the $\delta^{13}C$ values of speleothem calcite have been ascribed to climate-driven changes in vegetation (e.g., C3 versus C4 dominated plant assemblages) in arid regions (McDermott, 2004). In these regions, relatively large shifts in $\delta^{13}C$ can occur because soil respired CO_2 in equilibrium with a C3 dominated plant assemblage has $\delta^{13}C$ values in the range of -26 to -20‰, while that in equilibrium with C4 vegetation is significantly heavier ($\delta^{13}C$ of -16 to -10‰). These differences are preserved as distinctive ranges in $\delta^{13}C$ in secondary carbonates: typically -14 to -6‰ for carbonates deposited in equilibrium with CO_2 respired from C3 plants, and -6 to +2‰ for that from C4 plants (McDermott, 2004).

However, many temperate-zone speleothems also show carbon isotope values higher than -6‰ (McDermott, 2004). These values are higher than those predicted to be in equilibrium with the prevalent C3 vegetation in temperate regions. It is believed that complete isotopic equilibration may not occur between soil CO_2 and the percolating H_2O in situations where the soil-water residence times may be relatively short, resulting in water with a component of (isotopically heavier) atmospheric CO_2 in solution. Other explanations for relatively heavy carbon isotope signatures include processes like evaporation, rapid degassing of cave drip-waters, kinetic fractionation, CO_2 degassing of drip-waters and consequent calcite precipitation in the vadose zone above a cave (McDermott, 2004). Studies have shown an increase in altitude and slower drip rates also reveal more positive carbon isotope values (Johnston et al., 2013).

On the other hand, stalagmites deposited during the late glacial in Villars, 260 km northwest of Mélagues, exhibit $\delta^{13}C$ values that are much higher than those deposited during the Holocene (Genty et al., 2003). These differences were attributed to changes in biological soil activity conditions, which influence the carbon isotope signature of stalagmites. Consequently, degradation of vegetation and soil will decrease the biogenic CO_2 production. When the biogenic CO_2 dissolved in seepage water increases on the other hand, $\delta^{13}C$ values in speleothems are lower and related to warm periods (Genty et al., 2003). This interpretation implies that periods of climatic amelioration promote the production of biogenic CO_2, resulting in isotopically lighter carbon isotope ratios in the speleothem calcite.

The driver for speleothem precipitation is the difference in CO_2 between the soil/upper epikarst and the cave system, since precipitation of calcite occurs as soon as water encounters lower pCO_2 in air circulating in the cave (Fairchild and McMillan, 2007). During prior calcite precipitation (PCP) and thus before the forming of the stalagmite, calcite is deposited from the percolating epikarst water before entering the cave as drip water. This PCP process mostly occurs during drier periods, when drip rates are slow, cave air pCO_2 is low and aerated zones become more important in the epikarst (Oster et al., 2012; Van Rampelbergh et al., 2015). PCP tends to be enhanced by two processes: (1) seasonal falls in CO_2 in the cave air and (2) seasonally low water flows, leading to more extensive penetration of air into the aquifer (Fairchild and McMillan, 2007).

Research in the Han-sur-Lesse epikarst in Belgium suggests that prior calcite precipitation causes a simultaneous increase in the $\delta^{13}C$ and in the Mg/Ca and Sr/Ca composition of the drip water and speleothem calcite (Van Rampelbergh et al., 2015). Drier periods in this particular cave are caused by lower winter recharge periods, resulting decreased drip discharge and increased $\delta^{13}C$ values are interpreted to reflect drier and most probably also colder winter periods. Furthermore, during periods of lower drip discharge, PCP will occur and further increase the $\delta^{13}C$ values. More positive $\delta^{13}C$ values thus reflect lower soil activity and increased PCP during drier (and colder) winter periods (Van Rampelbergh et al., 2015).

Additionally, an increase in precipitation amount might also cause a decrease in the $\delta^{13}C$ value of speleothem calcite by increasing soil moisture content and soil respiration rates or by reducing water-rock interactions, thereby reducing the amount of $\delta^{13}C$-enriched carbon derived from the host limestone (Van Breukelen, 2009). Finally, both equilibrium and kinetic effects can affect/perturb the $\delta^{13}C$ of the precipitated calcite during progressive outgassing of CO_2 into the cave atmosphere (Schwarcz, 2007).

1.7.2. Oxygen isotopes

Variations in the $^{18}O/^{16}O$ ratio in water and oxygen-bearing minerals have been widely used as proxies for various environmental records, especially temperature. $CaCO_3$ can isotopically exchange with water: $1/3\ CaC^{18}O_3 + H_2{}^{16}O \leftrightarrow 1/3\ CaC^{16}O_3 + H_2{}^{18}O$, while the equilibrium constant for this reaction only depends on temperature (Schwarcz, 2007). The $\delta^{18}O$ value of speleothem carbonate precipitated under isotope equilibrium is hence controlled by two factors: (1) the oxygen isotope composition of cave drip water and (2) the temperature at which the precipitation occurs (Van Breukelen, 2009). Therefore, if a sample of $CaCO_3$ is precipitated in isotopic equilibrium with water of known $^{18}O/^{16}O$ ratio, it is possible to reconstruct the temperature at the time of precipitation. It is very difficult to discriminate between the temperature and other factors influencing the $\delta^{18}O$ of precipitation, such as amount effect, changes in moisture source and transport pathways (Verheyden et al., 2014). However, the change in precipitation effect is, in most cases, predominant and, thus, the $\delta^{18}O$ of speleothems is in practice interpreted mainly as changes in $\delta^{18}O$ of precipitation (Verheyden et al., 2014).

Orographic and altitude effects also affect the $\delta^{18}O$ value in precipitation and thus in speleothems. A decrease in oxygen isotope values of precipitation and cave dripwater is observed with an increase in altitude or distance from the ocean (continental effect), since the heavier isotope is preferentially precipitated, especially as the air rises and cools (Johnston et al., 2013; Lachniet, 2009). However, little work has explored the spatial variations in isotopic effects as preserved in speleothem $\delta^{18}O$ values, especially in our study region. Speleothems should record the altitude effect in their mean $\delta^{18}O$ composition of multiple samples collected within a region (Lachniet, 2009). Orographic distillation of air masses, as they traverse a high mountain range, may result in a pronounced "isotopic rain shadow", which leads to drier areas and more negative $\delta^{18}O$ values on the lee-side of the barrier (Blisniuk and Stern, 2005). Furthermore, $\delta^{18}O_{ct}$ values (the oxygen isotope composition of calcite in speleothems) for European Holocene speleothems decrease as a function of distance from Atlantic Ocean (longitude), which is a result of a progressive rainout effect, while the general Atlantic moisture circulation pattern does not seem to have changed on a multi-decadal timescale during the Holocene (McDermott et al., 2011). Therefore, as the amount of rain increase, lower $\delta^{18}O_{ct}$ values can be observed, while relatively high $\delta^{18}O$ values are associated with low precipitation amounts. More positive $\delta^{18}O$ values correspond to drier periods in a study in the Han-sur-Lesse cave in Belgium and thus reflect the amount effect (Verheyden, 2001).

However, it is essential that an isotopic equilibrium between the water and dissolved and precipitated carbonate phases has been established in order for speleothems to reliably track changes in the $\delta^{18}O$ values of the cave drip waters, since kinetic fractionation in speleothems deposited at disequilibrium results in isotope covariations (Hendy, 1971). Speleothems form at oxygen isotopic equilibrium with drip waters if the mode of deposition was by relatively slow outgassing of CO_2 from the drip water (Schwarcz, 2007). These equilibrium depositions are widely found deep inside long (>1 km) caves or in recently opened, formerly sealed cavities, where relative humidity was ~100% and where lack of significant movement of air resulted in high partial pressure of CO_2, resulting in a slow outgassing of drip water. The discovery of this means of recognizing speleothems deposited at equilibrium opened up the possibility of using variations of $^{18}O/^{16}O$ ratios in calcite in speleothems as a paleothermometer. Far (>100-500 m) from the entrances of most caves, the temperature remains constant seasonally and approaches the annual surface temperature above the cave. Therefore, a paleotemperature record from an equilibrium speleothem would provide a record of past temperatures on the surface for the duration of growth of the speleothem (Schwarcz, 2007).

Many studies have laid their hands on the question what the best paleotemperature equation is. Several factors have to be taken into consideration, most importantly the type of material. The equation most relevant for this study is the one by Kim and O'Neil (1997), since the Montagne Noire

speleothem mostly has an inorganic mineralogy. In order to compare the differences in paleotemperature equations also the formula by Craig (1965), based on mixed organic calcite and aragonite, is used. A compilation study by McDermott et al. (2006) has shown this equation generally gives the more accurate results, since the Kim and O'Neil (1997) equation leads to temperatures that are several degrees Celsius too low. However, in order to determine an accurate paleotemperature it is necessary to have oxygen isotope values from both the calcite ($\delta^{18}O_{ct}$) and the drip water from which it was precipitated ($\delta^{18}O_w$).

1.7.3. Hydrogen isotopes and fluid inclusions

It has been recognized since the 1970s that speleothems contain small amounts of seepage water trapped in small cavities in the speleothem calcite, so-called fluid inclusions, which make up on average about 0.1% of the weight of speleothems (Van Breukelen, 2009). The ability to analyse stalagmite fluid inclusion $\delta^{18}O$ values eliminates the uncertainty associated with reconstruction of $\delta^{18}O_w$ and thus allows for the reconstruction of independent speleothem growth temperatures based on paired fluid inclusion and host calcium carbonate oxygen isotope values. Fluid inclusion isotope values in stalagmites provide temporal records of rainfall isotope variation which in turn can be related to changing rainfall patterns through time, since cave drip water, and thus fluid inclusion water, is believed to reflect the isotope composition of local rainfall recharging the cave aquifer (Van Breukelen et al., 2008; Van Breukelen, 2009).

The petrographic and SEM microscope analyses (Fig. 3.9) also reveal the presence of fluid inclusions in the calcite of the speleothem used in this study. If the mineralogy of the speleothem and fluid inclusions are interpreted to be primary and, thus, did not form after the deposition of the speleothem, it confirms that the fluid inclusion isotope composition is undisturbed since the time of its formation (Van Breukelen, 2009).

In this study, the $\delta^{2}H$ and $\delta^{18}O$ in fluid inclusions were measured. This data has been compared to the so-called Global Meteoric Water Line (GMWL; Fig. 3.5). In the atmospheric hydrological cycle, hydrogen and oxygen isotopes have a fixed relationship, expressed as the GMWL (Dansgaard, 1964). The slope of the GMWL is defined by the Rayleigh effect and globally described by the equation $\delta^{2}H = 8 \cdot \delta^{18}O + 10$ (Craig, 1961). This relationship of isotopes in cave seepage and fluid inclusion water is useful to investigate whether secondary effects on the oxygen isotope composition of inclusion water have taken place (Van Breukelen, 2009). If the fluid inclusion oxygen isotope composition moves away from the GMWL, by oxygen isotope exchange between inclusion water and the surrounding speleothem carbonate, erroneous paleotemperature calculations will result. Hydrogen isotopes of fluid inclusion water cannot exchange with the host carbonate, since $CaCO_3$ does not contain any hydrogen molecules (Van Breukelen, 2009). In 3.2. Fluid inclusions, cross plots of hydrogen and oxygen isotope data of fluid inclusion water (Fig. 3.5) are used to determine whether they fall on the GMWL as indicator of secondary oxygen isotope exchange (Van Breukelen, 2009). The oxygen isotope composition of rainwater is mainly affected by temperature and rainfall amounts, which complicates the quantitative interpretation of fluid inclusion isotope data (Van Breukelen, 2009). However, by combining the $\delta^{18}O$ values of fluid inclusion water ($\delta^{18}O_w$) and its surrounding calcite ($\delta^{18}O_{ct}$), independent paleotemperatures can be calculated based on the known temperature dependency of $\delta^{18}O$ fractionation between speleothem calcite and precipitating water. This makes it possible to distinguish between the effects of temperature and rainfall $\delta^{18}O$ values on the isotope patterns in stalagmite calcite.

1.7.4. Colour analyses

The precise controls on the relation between the colours and geochemical composition in speleothems are poorly understood, but a few suggestions are proposed here. Thinner and darker calcite layers form under slower growth, since the growth rate is primarily dependent on the discharge amount and the cave seepage water calcium ion concentration (Van Rampelbergh et al., 2015). The discharge is expected to be lower during (seasonally) drier and colder periods, while the cave seepage water calcium ion concentration itself depends on mainly two factors:

1. The soil pCO_2, which is expected to increase during warm and wet periods. Such an increase causes the amount of CO_2 dissolved in water to raise, so calcium carbonate is more easily dissolved and the calcium ion concentration in seepage water will thus increase.
2. The intensity of prior calcite precipitation (PCP), which mostly occurs during dry and cold periods. PCP decreases the Ca^{2+} concentration of the drip water due to precipitation of calcite in the epikarst. During these dry periods, soil activity will decrease and PCP will increase, leading to lower calcium ion concentrations in the drip water (Van Rampelbergh et al., 2015).

A lower calcium ion concentration and a lower drip recharge during drier and colder periods will, thus, cause slower calcite deposition and consequently thinner, more densely packed and darker and/or disturbed layers.

However, the presence of the brown layers suggests wetter periods due to higher concentrations of organic matter, while colourless calcite deposits form in drier periods (Asrat et al., 2008; Baker et al., 2007; Baker et al., 2008). However, this interpretation might not be trustworthy, since the oxygen and carbon isotope measurements of the used speleothems possibly indicate non-equilibrium conditions during deposition.

1.7.5. Petrographic microscope analyses

Carbonate is precipitated from a thin fluid layer. This layer is evenly distributed over the stalagmite and CO_2-degassing makes carbonate precipitation possible. Layer by layer, the stalagmite is built up, although this is not visible in the crystal structure itself, only by layering of organics, clay particles and fluid inclusions (Van Breukelen, 2009).

Differences in crystal structures indicate variable conditions during or after the formation of the stalagmite. Speleothem calcite fabrics provide valuable information on post-depositional phenomena (diagenesis), such as phase transformations, dissolution and re-precipitation processes, which may alter the original geochemical signal (Frisia, 2015). Fabrics develop under certain environmental parameters, in which fluid flow and presence of impurities are the most important. These parameters influence a certain spatial arrangement of crystals with a dominant form. The speleothem fabrics can be grouped in five main groups: columnar types, dendritic, micrite, microsparite and mosaic calcite (Frisia, 2015). In this section, only the fabrics that are observed in the Montagne Noire speleothem are discussed. A general overview of the characteristics and environments of formation of the fabrics observed in the Montagne Noire speleothem is shown in figure 1.9.

Columnar compact and open

Columnar fabrics are characterized by competitive growth (geometric selection), whereby crystals compete growing away from an interface. The crystals with the greatest growth vector perpendicular to the substrate will be favoured, while those with the greatest growth vector orientated in different directions will be outcompeted. In this way, small crystals with seemingly “random” growth directions are observed above the interface, as proof of a nucleation episode (Frisia, 2015).

If the crystals form a compact aggregate with welded crystal boundaries and if intercrystalline porosity is not observable with an optical microscope, the fabric is columnar compact. If intercrystalline boundaries are marked by the presence of linear inclusions or pores, then the fabric is columnar open.

Open columnar fabrics, thus, may contain many inclusions, while elongation of calcite attributed to high Mg content. This fabric also indicates conditions of free growth and discharge variability (Frisia, 2015).

Kendall and Broughton (1978) were the first authors establishing a general model for the development of compact (complete coalescence of crystallite) and open (incomplete coalescence) columnar calcite. The first type forms from a thin film of fluid, under relatively slow drip rate and enhanced degassing conditions (enhanced cave ventilation), while the latter forms from a thicker film of fluid, under higher drip rate and less efficient degassing**.** Further research suggests that, in temperate climate settings, columnar fabric forms under relatively constant discharge, low (<0.35) calcite supersaturation state (SI_{cc}), low Mg concentrations in the dripwater (Mg/Ca ratio <0.3) and negligible presence of particulate and/or organic colloids (Frisia, 2015). More positive carbon isotope ratios values in the compact columnar laminae reflect enhanced degassing, typical of low drip rates combined with intense cave ventilation (Boch et al., 2011).

In conclusion, columnar compact and columnar open columnar fabrics result from growth processes that imply a combination of low/high drip rate and high/low degassing. The carbon isotope ratios in the two types may, thus, be more or less modified by kinetic effects. Additionally, a relatively low Mg/Ca ratio range measured to date in their parent waters (0 to 0.3) and trace element variability may likely reflect impurities trapped within intercrystalline spaces in the open type (Frisia, 2015).

Columnar elongated

Elongated columnar calcite fabric is common in flowstones developed from parent waters whose catchment intersected dolomitic or Mg-rich rocks. Thus, it seems plausible to hypothesize that elongated columnar type forms from constant drip, similar SI_{cc} but higher Mg/Ca ratios (> 0.3) than for columnar compact and open (Frisia, 2015).

Spherulitic type growth in columnar fabrics: columnar radiaxial

Radiaxial or fibrous calcite is a fabric that can be observed as a pattern of converging fast vibration directions, which is undulatory extinction converge away from the substrate (Fig. 1.7). This fabric forms through a mechanism typical of spherulitic growth, which implies splitting of a crystal into a number of units with slightly diverging lattice orientation. Overall, the presence of the columnar radiaxial fabric indicates that speleothems formed under conditions of at least constant flow and suggest that cave breathing or ventilation may result in kinetic modifications of the geochemical signals encoded in the fabric. It is reasonable to assume that the columnar fabrics with spherulitic type growth most likely develop from higher Mg/Ca ratio dripwater (≥0.4 and ≤3) and SI_{cc} (≥0.3 and ≤0.5) than those required for the development of elongated, compact or open columnar fabrics (Frisia, 2015).

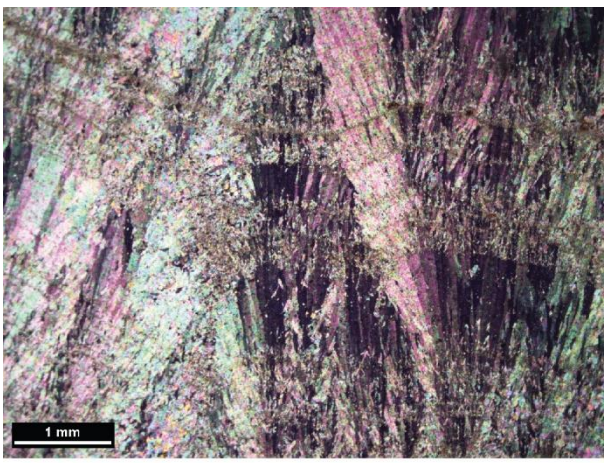

Figure 1.7. Photograph of thin section KM2-A, showing (columnar) spherulitic type growth.

The occurrence of this fabric seem to be typical in stalagmites and flowstones whose calcite Mg content is high, but still within the range of low-Mg calcite, typically from >10,000 to <30,000 ppm. However, the boundary conditions that shift the system from one that favours the development of elongated low-Mg calcites, to one that favours that of spherulitic-type fabrics and finally the precipitation of aragonite depend on a series of variable factors, such as temperature, SI_{cc} and Mg/Ca ratio, the carbonate ion concentration and the presence of organic compounds in the parent waters (Frisia, 2015).

An increase in Mg concentration in speleothems is commonly related to dry periods. During these periods, drip rate is low, Mg, Sr and Ba concentration should increase and $\delta^{18}O$ values of the drips should become more positive (Orland et al., 2014). It is reasonable to assume that spherulitic type growths in columnar fabrics are indicative of Prior Calcite Precipitation (PCP) and/or prolonged water-rock interaction (WRI) in dolomitized aquifers during dry periods (Frisia, 2015).

Micrite

Micrite, commonly appearing dark or dark brown (Fig. 1.8), is one of the most intriguing speleothem fabrics, because experimental studies showed the precipitation of micrite commonly requires an exceptionally high number of pre-existing nuclei, high supersaturation and/or the presence of organic compounds. Mechanisms of micrite formation in continental environments in laminar calcretes and tufas implies a biotic intervention, such as precipitation mediated by cyanobacteria. Similarly, micrite fabrics are characterized by stromatolite-like structures in speleothems from the Swiss Alps that grew under a glacier. These structures mark periods of glacier retreat, highlighting that micrite could be used as a paleoglaciological proxy (Luetscher et al., 2011). Stromatolite-like micrite layers are also observed in Holocene stalagmites from a mid-altitude cave in the Dolomites and in Pliocene stalagmitic flowstones from the Nullarbor, where they coincide with reduction or cessation of the common abiotic speleothem growth processes (Frisia and Borsato, 2010; Frisia et al., 2012). Epifluorescence (UV) observations support the hypothesis that micrite fabric in stromatolite-like structures is related to organic compounds, microbial laminae and cave microbes-influenced formation of micrite. The appearance of micrite fabric has important implications for paleoclimate studies, since micrite layers may be associated with shifts to more positive values in the carbon isotope ratios. Micrite is thus interpreted as a possible result of microbial colonization of the speleothem surface during a relatively dry period (Frisia, 2015).

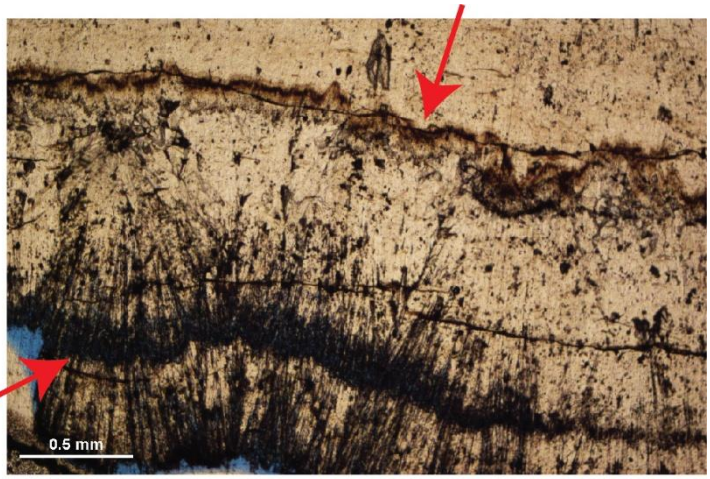

Figure 1.8. Photograph of thin section KM3, showing possible micrite layers (red arrows).

In addition, etching, biomechanical "micritization", and condensation-corrosion may all create micrite. Micrite associated with aragonite relicts has been considered a "destructive" fabric, formed through condensation-corrosion. However, aragonite needles in many speleothems are replaced by microsparite (see below), rather than by micrite. Therefore, it is unclear whether micrite fabric is a diagenetic product of condensation-corrosion or a primary fabric. Micrite associated with stromatolite-like structures is most probably a primary fabric, whereas micrite associated with aragonite can be diagenetic or not. Studies have shown it is reasonable to infer that micrite development in speleothems consisting of calcite is favoured by bio-mediation in a regime of relatively low discharge (Frisia et al., 2012; Frisia, 2015).

Diagenetic fabrics: microsparite

Microsparite consists of crystals >2 µm and <30 µm in diameter arranged in a mosaic, but its origin is still uncertain. A model for the genesis of microsparite (Frisia, 2015) suggest the microsparite fabric is inferred to be the product of aggrading neomorphism of micrite. Neomorphism describes the in-situ transformations of a mineral in itself (replacement of calcite by calcite) or by a polymorph (replacement of aragonite by calcite). These transitions are believed to take place through dissolution

of the “precursor” on one side of a film of fluid and precipitation of the neomorphic phase on the other side of the film. The replacement of micrite by low Mg-calcite microsparite is most probably a process of aggrading neomorphism and driven by the instability of very small crystals with high surface to volume ratio. The crystal size has to be extremely small (<2 μm) in order to occur at the low temperatures, under which speleothems commonly form. Therefore, this is the case for micrite. Aggradation would occur when a flow of saturated solutions enters in contact with micrite, which should imply a partial (or complete) opening of the system in order for microsparite to replace micrite (Frisia, 2015).

Microsparite is commonly observed in association with micrite in stromatolite-like layers and in dark, organic-rich laminae within stalagmites. In the latter case, organic matter oxidation may have promoted sin-depositional dissolution-re-precipitation processes, with little consequence on the preservation of original geochemical signals. The microsparite fabric is also typical as a replacement phase in aragonite needles, in the form of mosaics of calcite crystals that mimic single aragonite crystals morphologies. When discharge resumes after a dry period, the process of neomorphism with replacement of a precursor by calcite microsparite may be favoured, where either aragonite or micrite had previously formed. The process of microsparitization may also be influenced by the presence of inorganic or organic additives, which may control both the morphology of the precipitates and polymorphism. In speleothem forming environments, the presence of organic compound and microbes is bound to be ubiquitous. Accordingly, speleothem formation may not be dictated by sole inorganic processes. Reasonable to infer is that the development of microsparite is thus facilitated by the presence of organic compounds (Frisia, 2015).

Diagenetic fabrics: mosaic

If the process of diagenesis continues, a mosaic fabric might form in the speleothem. Each crystal in this fabric typically shows triple junctions and includes ghosts of dark needles, which are a distinguishing characteristic of calcite replacing aragonite. The occurrence of mosaic fabric has mostly been related to speleothem aragonite transformed into calcite. Mosaic calcite, however, has also been reported as the product of dissolution and re-precipitation of former low-Mg calcite. It is still unclear if mosaic calcite is the final product of neomorphism in a micrite → microsparite → sparite series in continental carbonates or a product of dissolution of columnar calcite and re-precipitation of mosaic calcite driven by influx of undersaturated waters causing dissolution of a pre-existing fabric, and re-precipitation of sub-euhedral crystals. In the Montagne Noire speleothem, the latter case would be expected when for example glacial meltwaters invaded cave systems during deglaciations. Another argument to support this is the abundance of calcite instead of aragonite. Mosaic fabric consisting of sparite, without evidences of former aragonite needles, should be considered a diagenetic product of dissolution and re-precipitation of any of the primary calcite fabrics, most probably of the most porous, like columnar open in the Montagne Noire speleothem (Frisia, 2015). In the studied speleothem, the mosaic structure should not be confused with the breccia deposits in the calcite, which are more rounded.

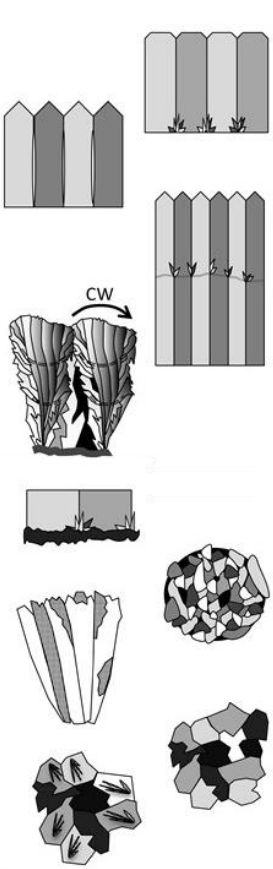

Type	Characteristics	Environment of formation
Columnar	l/w ratio <6:1; competitive growth at interfaces; straight to serrated boundaries; uniform extinction; common "flat" terminations or protruding rhombohedra terminations (~ 2µm high)	Relatively slow and constant drip; Slcc < 0.35; Mg/Ca <0.3; pH up to 8. 4; low impurity content
Columnar open	l/w ratio <6:1; competitive growth at interfaces; incomplete coalescence of crystals; high intercrystalline porosity, commonly linear; uniform extinction.	Drip rate > than in C; Slcc up to 0.35; Mg/Ca <<0.3; pH 7.5 up to 8.
Columnar elongated	l/w ratio > 6:1; competitive growth at interfaces; preferential growth of acute rhombohedron; incomplete coalescence of crystals; protruding terminations common; uniform extinction. May show lateral overgrowths, in particular in the presence of impurity-rich layers.	Drip rate constant; Slcc 0.1 to 0.4; Mg/Ca > 0.3.
Columnar radiaxial	Polycrystals l/w ratio > 6:1; undulatory extinction converge away from substrate when rotating table turned CW; split crystal growth; upward concave curvature.	Low drip rate or laminar flow; Slcc 0.5; Mg/Ca > 1.5; typical in stalagmites & flowstones formed in caves cut in dolomite
Micrite	Crystals < 2µm; stromatolitic-like structure; clotted structure. Common geometric selection above micrite layers.	Bio-influenced. Low flow/dry. Condensation/corrosion?
Microsparite	l/w ratio ~ 1:1; crystal size > 2µm < 30µm; commonly associated with micrite. Fabric-destructive replacement.	Diagenesis. Aggrading neomorphism (micrite to microsparite)
Replacive microsparite	l/w ratio ~ 1:1; Crystal size > 2µm < 30µm; retention of aragonite fabric.	Diagenesis. Mimetic replacement
Mosaic calcite	l/w ratio ~ 1:1; crystal size > 30µm. Fabric destructive.	Diagenesis. If replacing calcite, no relicts of a former unstable phase are visible.
Mosaic calcite with aragonite needles	l/w ratio ~ 1:1; Crystal size > 30µm; Fabric destructive; preserves relicts of aragonite, commonly needles.	Diagenesis. Commonly related to the transformation of speleothem aragonite into calcite

Figure 1.9. Indication of the characteristics and environments of formation of the fabrics observed in the Montagne Noire speleothem. Modified after Frisia (2015).

2. Methodology

2.1. Materials

For this study, a ±18 cm long slab was cut out of a stalagmite. Its width decreases from ±7.5 cm at the top to ±3 cm at the bottom. The polished stalagmite slab displays a succession of dark brown to milky white laminae (Appendix IV). The speleothem was taken from a karstic cavity located in a road in Montagne Noire, 2 km to the NW of Mélagues (Aveyron, Midi-Pyrénées, Occitanie, France; Fig. 1.1). The stalagmite was cut longitudinally, after which a polished slice of about 1.2 cm thick was used to drill samples for stable isotope analyses.

Thin sections from the other half of the speleothem were used for petrographic microscope imaging, scanning electron microscopy (SEM) and energy dispersive X-ray spectroscopy (EDS). Additionally, ±0.8 cm wide and 1.2 cm thick samples were drilled for the stable isotope analyses of stable isotope signatures in fluid inclusions. All analyses, except X-ray diffraction (XRD), for which different sized samples were used (Fig. 2.4), were performed at the Vrije Universiteit (VU; Amsterdam, The Netherlands).

2.2. Methods

2.2.1. Stable isotopes

Samples for the stable isotope analyses were drilled with a Proxxon hand held drill tool at 1 millimetre spatial resolution along the growth axis of the speleothem (Appendix IV). These powdered samples were measured for their $\delta^{18}O$ and $\delta^{13}C$ values on a Finnigan DeltaPlus isotope-ratio mass spectrometer (IRMS) equipped with a Finnigan GasBench II preparation device with a 1-2 mm spatial resolution.

CO_2 was generated from carbonate samples by dissolution with water-free phosphoric acid (100% H_3PO_4). During this process, the temperature of the autosampler sample tray block was kept constant at 45 ^{o}C. All sample tubes (Fig. 2.1) were flushed with the inert and noble gas helium to make sure no atmospheric gasses are measured. Possible reactions are:

(1) $2H_3PO_4 + 3CaCO_3 = 3CO_2 + 3H_2O + Ca_3(PO_4)_2$

(2) $2H_3PO_4 + CaCO_3 = CO_2 + H_2O + Ca(H_2PO_4)_2$

(3) $H_3PO_4 + CaCO_3 + H_2O = CO_2 + 2H_2O + CaHPO_4$

The mixture of CO_2 and helium from the headspace, that carries the carbon and oxygen isotopic signature of the sample, is analyzed by IRMS using the Finnigan DeltaPlus. A CO_2 monitor gas with known isotopic ratio is also analyzed during each measurement to determine the $\delta^{13}C$ and $\delta^{18}O$ values of the sample. A sample size correction is done for every run using the in-house carbonate standard of the stable isotope lab of the Vrije Universiteit Amsterdam (VICS). The internationally used standard IAEA-603, with values of +2.46‰ VPDB for $\delta^{13}C$ and -2.37‰ for $\delta^{18}O$ VPDB, is measured as a control standard. These control standard values show a quite high average standard deviation of 0.10‰ for $\delta^{13}C$ and 0.14‰ for $\delta^{18}O$ (Appendix II).

All samples and standards are corrected for the sample-size effect using their peak-heights (mV Amplitude 44). After this correction, measurements having voltages between 1000 and 10.000 mV are considered to be reliable. Samples outside this range are measured again and/or both adjacent samples are used to obtain reliable isotope values (Appendix II). Both $\delta^{18}O$ and $\delta^{13}C$ are reported in ‰ relative to Vienna PeeDee Belemnite (VPDB).

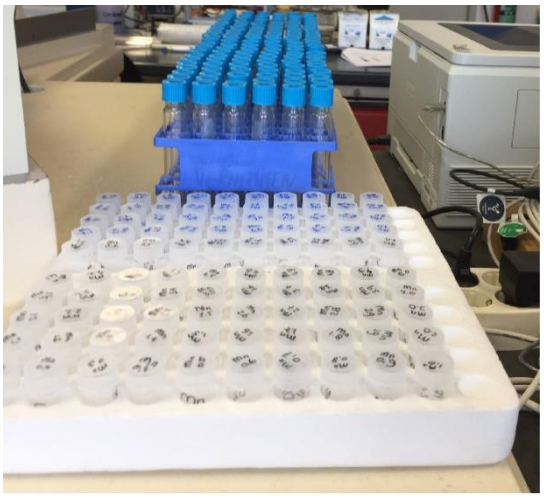

Figure 2.1. Photograph of sample tubes before (white) and during (blue) analyses.

2.2.2. Fluid inclusions

Prior to the actual fluid inclusion measurements used in this thesis, a few tests were performed on the Amsterdam Device 2.0. These tests showed the system, unfortunately, was not able to meet the requirements for correct and reliable measurements yet, so it was decided to use the first version of the Amsterdam Device. For more information about this device and its procedures, see 3.2. Fluid inclusions, Appendix II and Van Baal et al. (2017).

Samples for the fluid inclusion analyses were first dried in a 60 °C oven for at least a day in order to remove any non-speleothem water absorbed from the surface of the sample, which could have 'contaminated' the sample. The samples were then crushed in the Amsterdam Device 1.0 to measure $\delta^{18}O$ and $\delta^{2}H$ values of the fluid inclusions. The Amsterdam Device 1.0 (Fig. 2.2) is connected to a ThermoFinnigan Thermal Combustion-Elemental Analyzer (TC-EA), which is a continuous-flow pyrolysis furnace. The Amsterdam Device 1.0 works with an IRMS, unlike the Amsterdam Device 2.0, which is connected to a cavity ring-down spectroscometer (CRDS). The main adaptation made to the standard TC-EA configuration is the addition of a crusher and cold trap unit, which is connected to the carrier gas inlet at the top of the TC-EA reactor tube (Vonhof et al., 2006). After the procedure described by Vonhof et al. (2006) was completed (Appendix II) and subsequent $\delta^{18}O/\delta^{2}H$ values of multiple injections of standard water were stabilized (in order to reduce the memory effect), the sample was crushed semi-manually and then measured. In order to calculate the values for correction of both isotope values, a few more standard water injections were measured afterwards and then compared to the data from the crush and stabilized standard water values from before the crush. This resulted in data reflecting the hydrogen and oxygen isotope values of the fluid inclusions trapped in the sample, expressed in ‰ relative to Vienna Standard Mean Ocean Water (V-SMOW). The analytical uncertainty (1σ) of the fluid inclusion isotope analyses for this device is <1.5‰ for $\delta^{2}H$ and <0.3‰ for $\delta^{18}O$ (Vonhof et al., 2006; Vonhof et al., 2007).

In order to calculate the paleotemperature, which provides a record of past temperatures on the surface for the duration of growth of the speleothem, two equations have been used. In the general equation $T(°C) = a + b(\delta_c - \delta_w) + c(\delta_c - \delta_w)^2$, Craig (1965) and Kim and O'Neil (1997) use different values for a, b, and c: respectively 16.9, -4.2 and 0.13 for Craig (1965) and 16.1, -4.64 and 0.09 for Kim and O'Neil (1997). The δ_c and δ_w resemble the oxygen isotope values of, respectively, the speleothem calcite and water, both in ‰ relative to Vienna PeeDee Belemnite (VPDB). Since the isotope data of the fluid inclusions is measured relative to V-SMOW, a correction is applied and 0.20‰ is subtracted from the δ_w value for the Craig (1965) equation, and 0.27‰ for the one by Kim and O'Neil (1997). For further information about the differences and use of both paleotemperature equations, see 4. Discussion or Bemis et al. (1998).

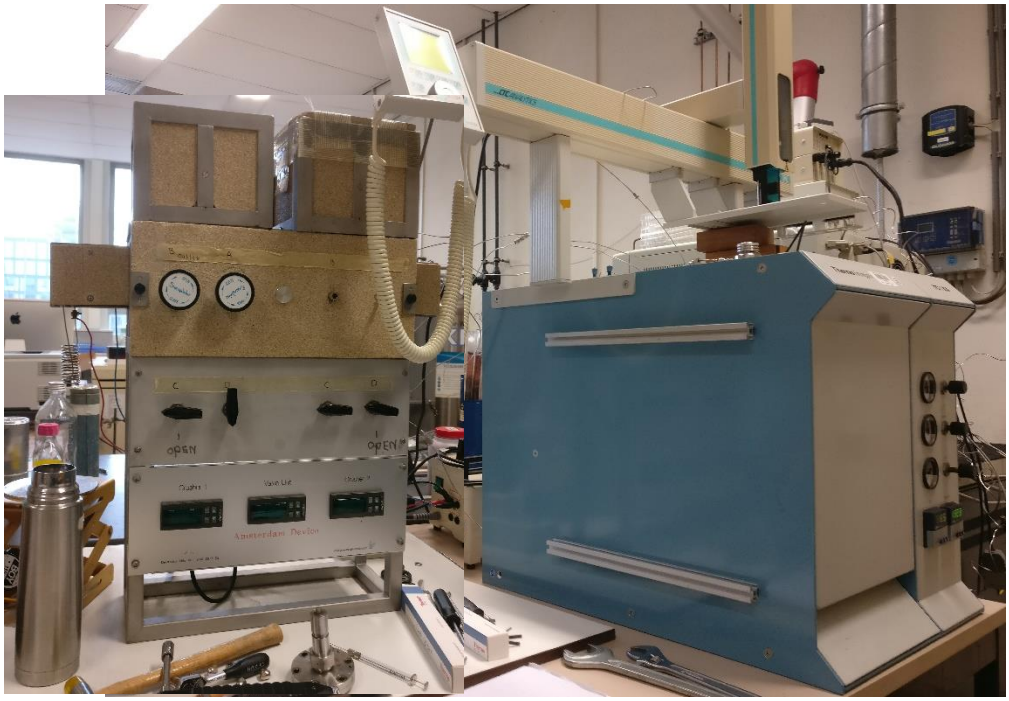

Figure 2.2. Photograph of the setup of the Amsterdam Device 1.0, with cold trap, heater and crusher (left) and the ThermoFinnigan TC-EA (right).

2.2.3. Colour analyses

Scans at 1200 dpi and 2400 dpi resolutions were made of the stalagmite using an Epson Perfection V700 Photo scanner to visualize the stalagmite itself and to analyse differences in RGB (Red, Green, Blue) intensities. The resulting intensity graph can be used to compare the colours/lamination with the isotopic composition of the speleothem. The script shown in Appendix II was used in Matlab R2017a in order to import the image, extract a colour data record from a transect along the growth axis of the stalagmite.

Other software programs that have been used to gather and/or process data in this project include EndNote, Google Earth/Maps, Grapher 6, Isodat Workspace/Acquisition/Instrument Control, Past 3.15 and Microsoft Excel.

2.2.4. Petrographic microscope analyses

Petrographic images of thin sections of the stalagmite were made using a Nikon Eclipse 50i POL microscope with different objectives and magnification levels.

2.2.5. Scanning electron microscopy (SEM) and energy dispersive X-ray spectroscopy (EDS)

Two thin sections (KM1-A and KM3) were first carbon coated three times each by a JEOL JEC-530 Auto Carbon Coater for 5 seconds with 4.5 Volt. Copper tape was applied to the thin sections (Fig. 2.3) to decrease e.g., charging. For both analyses, a JCM-6000 Benchtop Scanning Electron Microscope with its supplied standard hard- and software was used with the following settings on different magnification levels: high-vacuum mode, backscatter signal, 15 kV accelerating voltage, standard filament current and standard probe current. Screenshots of the SEM images were made after initializing the auto-adjustment process of focus, stigma and brightness. Depending on the resulting view, these three functions may have been changed manually.

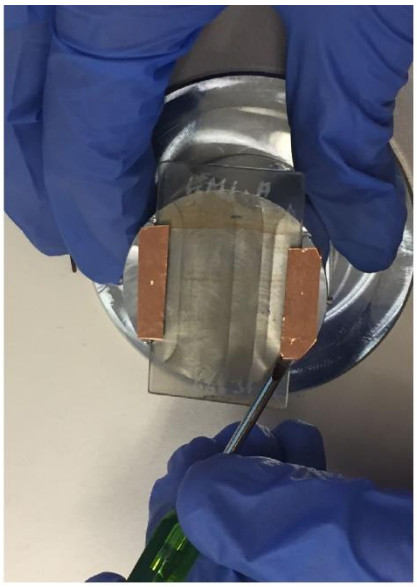

Figure 2.3. Photograph of the preparation for SEM/EDS analyses of a thin section.

After a sufficient SEM image was produced, the EDS aperture on top of the machine was turned clockwise in order to produce accurate EDS analyses. The X-ray intensities were then measured by counting photons, while the precision was limited by statistical error. The counts per second, displayedon the screen during the measurement, should be higher than 3% in order to give accurate results. After 100 seconds the measurement, quantitative and qualitative analyses were completed, resulting in tables and graphs showing the most abundant elements and oxides for the chosen image or spot. For quantitative analyses, a background correction was applied using a digital filter, peak overlap correction, K ratio calculation, ZAF correction (standard specimen spectrum) and $\phi(\rho z)$ correction.

2.2.6. X-ray diffraction analyses (XRD)

The mineral composition of the different parts of the speleothem (Fig. 2.4) were measured on the X-ray diffraction service at the ICTJA-CSIC in Barcelona, Spain. The XRD analyses were carried out on sample powders. Samples were analysed on the Bruker-AXS D8-A25 Advance XRD Service, which is equipped with a Cu X-ray tube and a Position Sensitive Detector (PSD) from LynxEye. Data was processed with the DIFFRACplus software, in combination with Crystallography Open Database (COD) and Powder Diffraction File (PDF-2) databases for phase identification. Quantitative mineral compositions were calculated with the Rietveld method (Young, 1993) by making use of TOPAS 4.2 software. Dolomite mineral phases are identified by ordering peaks at {101}, {015} and {021} and lattice parameters determining the dolomite crystal lattice.

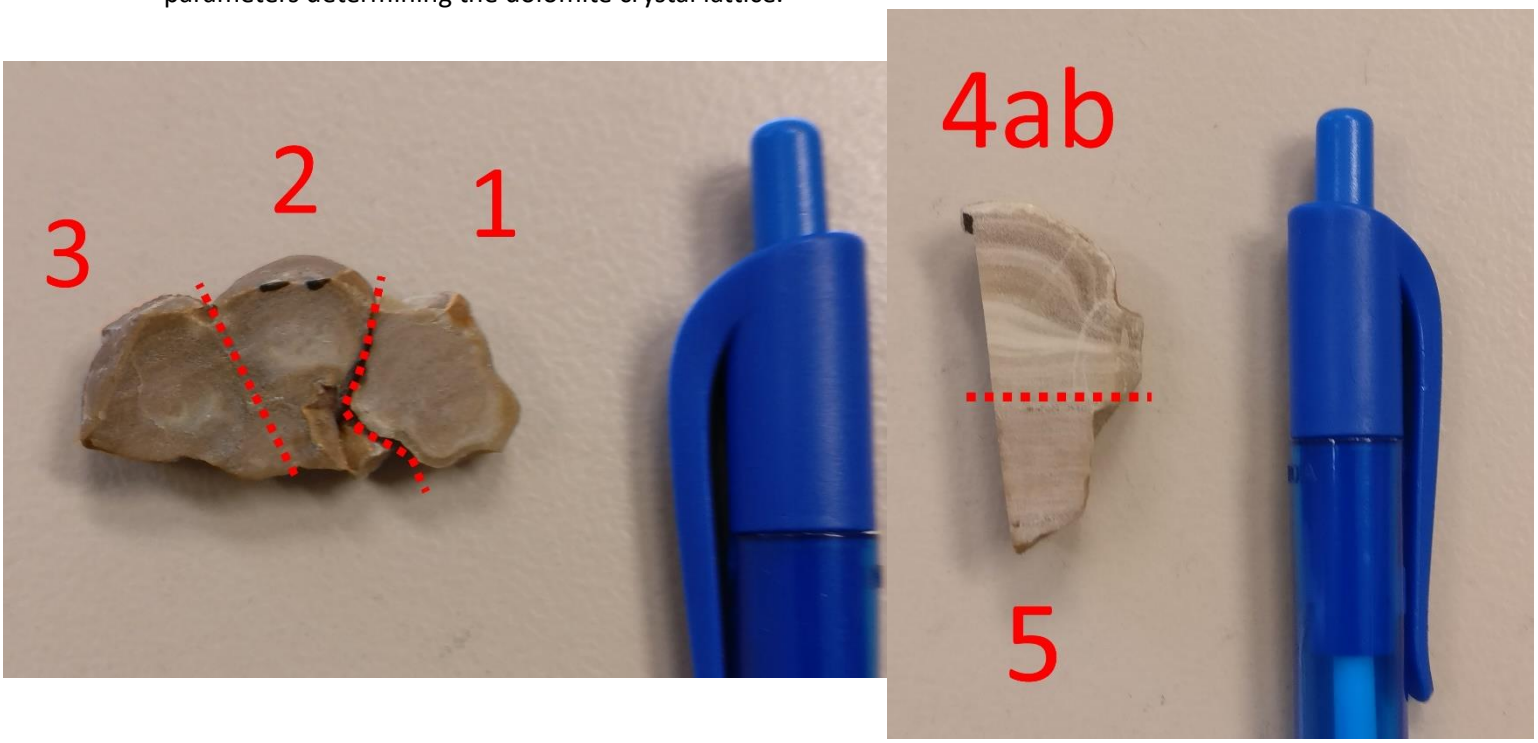

Figure 2.4. Photographs of the uncrushed samples for the XRD analyses. The red dotted lines indicate the borders between the sample numbers in the original material.

3. Results

3.1. Stable isotopes

The high resolution record of oxygen isotope values throughout the stalagmite shows a maximum variation of 1.91‰, while $\delta^{13}C$ shows a 3.23‰ maximum variation (Fig. 3.1). The average value is -9.36‰ ($1\sigma \approx 0.55$) for $\delta^{13}C$ and -4.38 ‰ ($1\sigma \approx 0.37$) for $\delta^{18}O$. Individual standard deviations of the measurements range from 0.02 to 0.23‰ for carbon and 0.02 to 0.20‰ for oxygen isotope values (Appendix III).

Relatively negative $\delta^{18}O$ values occur at 0.5, 1.3, 8.3-8.9, 9.9, 12.1-12.3 and 16.7-16.9 cm depth, while less negative values are measured at 0.8, 2.2, 4.1-4.3 and 10.1-10.9 cm depth. Carbon isotope values seem to remain more constant with depth, since values remain mostly between 9 and 10‰, with exception of less negative values at 0-1.1, 1.5-1.7, 2.9, 10.1-10.5, 11.3-11.5 and 18.1 cm and a single more negative value at 11.7 cm depth (Fig. 3.1).

Correlation plots of the stable isotopes are illustrated in figure 3.2. There is no relationship between the measured $\delta^{18}O$ and $\delta^{13}C$ values ($R^2 \approx 0.0055$). Major coupled increases with carbon isotopes are observed from 0.5, 2.0, 9.7 and 16.7 cm depth, while major coupled decreases occur from 1.1, 2.2, 2.9, 3.7, 4.3, 7.3, 11.9, 13.3, 15.5 and 16.5 cm depth. Therefore, coupled decreases are observed more frequently and abruptly.

A REDFIT spectral analyses for $\delta^{13}C$ shows cyclicity at a frequency of 3.3, 3.6 and 5.1 mm at a significance level of 1% (99% confidence level) and every 3.7 mm at a significance level of 5% (95% confidence level), while $\delta^{18}O$ only shows cycles at a length of 3.0 and 119.3 mm at a significance level of 1% and at intervals of 3.1 and 3.8 mm at a significance level of 5% (Table 3.1). The cyclicity in cm is calculated by 1/frequency of peaks higher than the significance levels of 0.01 and 0.05 (Fig. 3.3).

	Confidence level (%)	Spectral analyses peak (frequency)	Interval (mm)
$\delta^{18}O$	99	0.08	119.93
		3.35	2.98
	95	2.60	3.85
		2.64	3.79
		3.27	3.06
$\delta^{13}C$	99	1.97	5.08
		2.85	3.51
		3.06	3.27
	95	2.72	3.67

Table 3.1. Overview of confidence levels, frequencies and cyclicities for both stable isotopes.

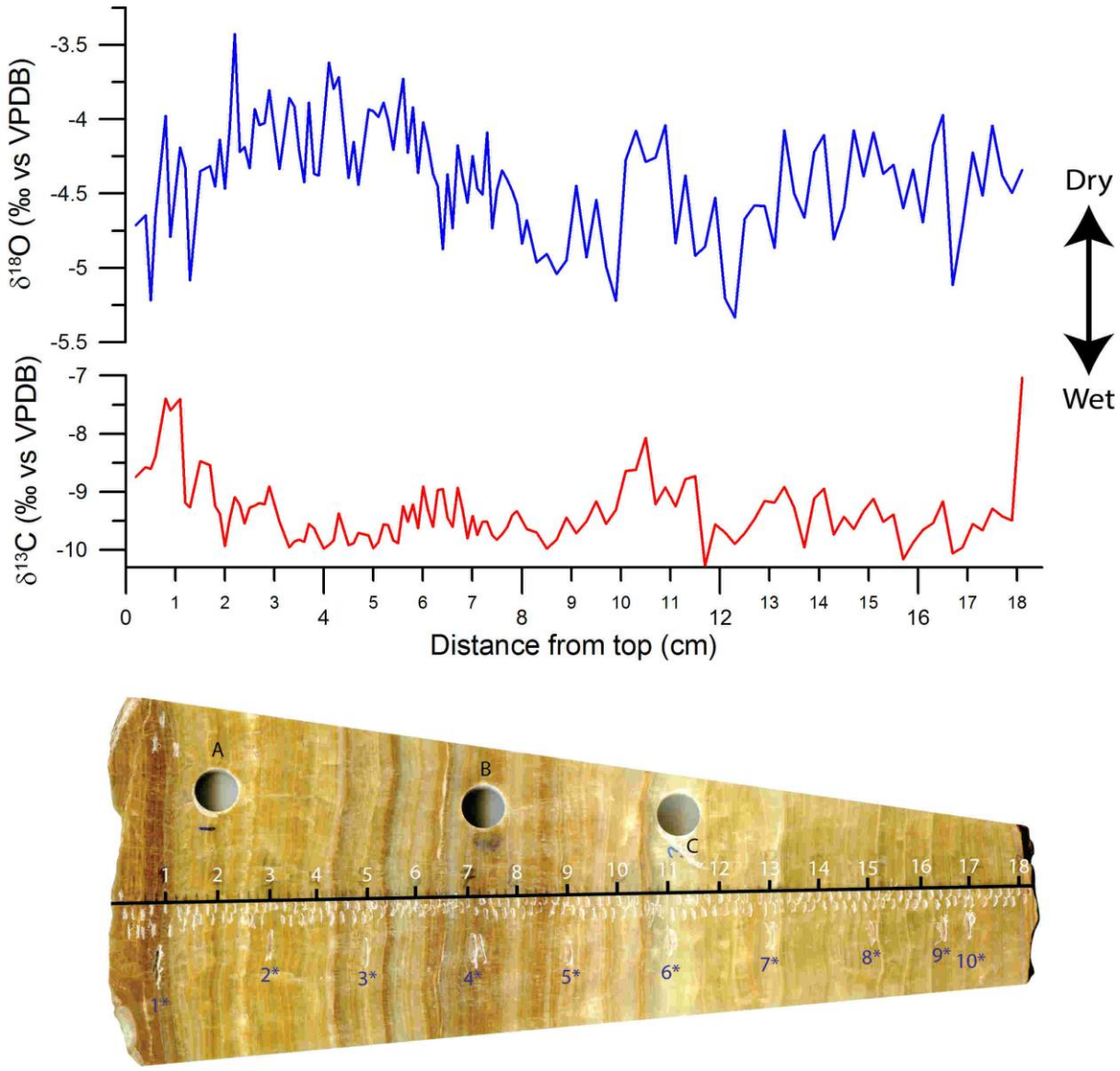

Figure 3.1. Stable isotope ($\delta^{18}O$, $\delta^{13}C$) records of the Montagne Noire stalagmite vs. distance from top.

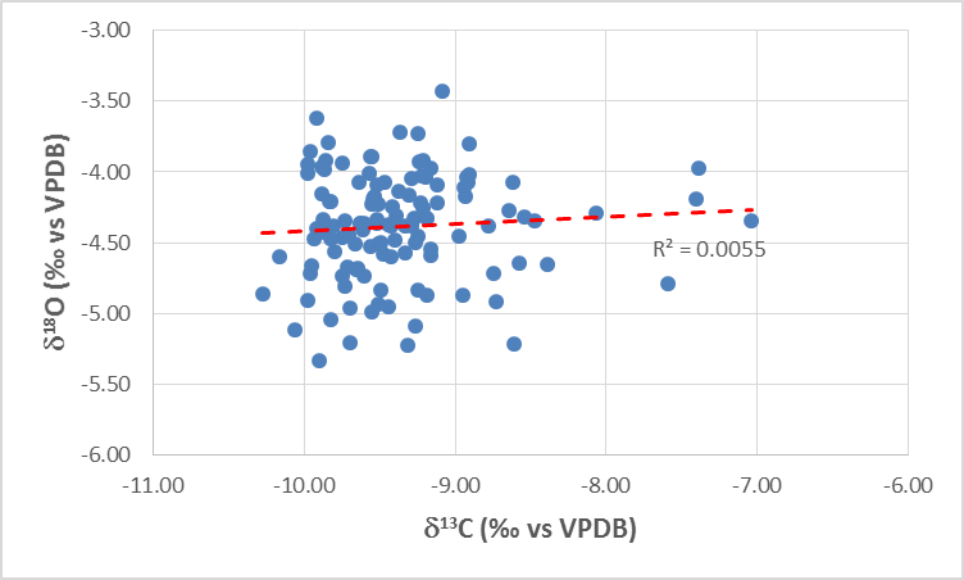

Figure 3.2. Cross plotted are the stable isotopes $\delta^{18}O$ and $\delta^{13}C$. The statistical fit of the linear correlation is indicated in the figure by the R-square.

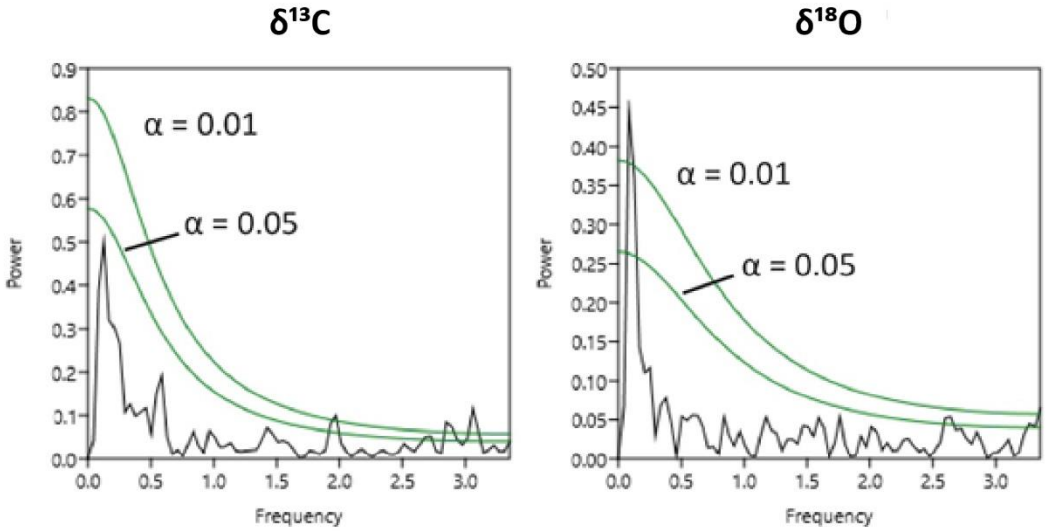

Figure 3.3. REDFIT spectral analyses for $\delta^{13}C$ (left) and $\delta^{18}O$ (right). Significance levels (α) are indicated by the green lines.

3.2. Fluid inclusions

At the start of this thesis, a few tests were performed on a new crusher system: the Amsterdam Device 2.0. The crusher is designed to measure stable isotopes in a Picarro, using laser Cavity Ring-Down Spectroscopy (CRDS) connected to a mechanical sample crusher with nitrogen as a carrier gas. This stable isotope crusher system is, like others, designed to extract water from fluid inclusions for analyses by a mass spectrometer (δ^{18} and $\delta^{2}H$). Since the development of this new crusher system is still in its early stages, factors such as noise and backgrounds still have to be investigated in more detail.

Although $\delta^{18}O$ and $\delta^{2}H$ show a clear correlation with a maximum expansion time of 2 minutes

after injection of a standard water sample with known isotope values, it remains unclear what exactly causes the sudden peak in H_2O (Fig. 3.4) at the time of writing. No clear relation between the H_2O peak and the expansion time is existent. Since it is preferred to have an approximately constant amount of H_2O at the start of such a measurement for reliable results and our research time was limited, it was decided to use the Amsterdam Device 1.0 for the fluid inclusion measurements in this thesis.

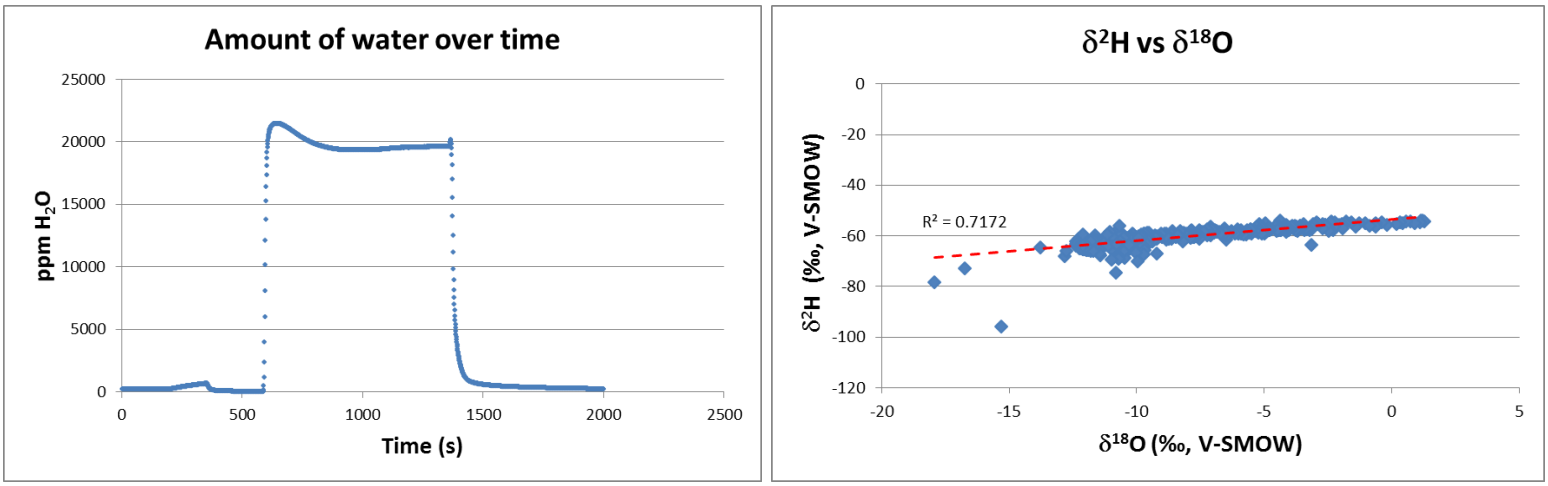

Figure 3.4. Concentration of H_2O before, during (abrupt increase/decrease) and after the measurement of the standard water sample (left) and $\delta^{18}O$ vs $\delta^{2}H$ cross plotted in the area of the measurement, in which the concentration of H_2O is higher than 10.000 ppm (right). The statistical fit of the linear correlation is indicated in the figure by the R-square.

Results from the Amsterdam Device 1.0 show ~4.11‰ variation in $\delta^{2}H$ values and ~0.18‰ in $\delta^{18}O$ values after corrections. The water yields from both analyses are relatively low (<0.1 µl) compared to fluid inclusions in other speleothems (De Bie, 2017; Van Breukelen, 2009), with the youngest sample displaying the lowest amount of water. Isotope values from the oldest part of the stalagmite plotted away from the Global Meteoric Water Line (GMWL), which is the average relationship between hydrogen and oxygen isotope ratios in rainfall, expressed as a worldwide average (Craig, 1965; Fig. 3.5). This was a sample with an even lower water yield than the other two, resulting in erroneous isotope values, as was confirmed by yield tests with an in-house water standard. The measurements from this sample were discarded for the discussion of the data. The values from the middle of the stalagmite plot more accurately on the Local Meteoric Water Line (LMWL; IAEA/WMO, 2013) from Avignon, ~150 km east of Mélagues, than the values from the sample of the top. In addition, the average annual hydrogen isotope composition in the precipitation around our study site is much lower than the $\delta^{2}H$ values observed in the studied speleothem (-38.12 ± 7.89‰ in Avignon vs. -28.34‰ at our study site; IAEA/WMO, 2013).

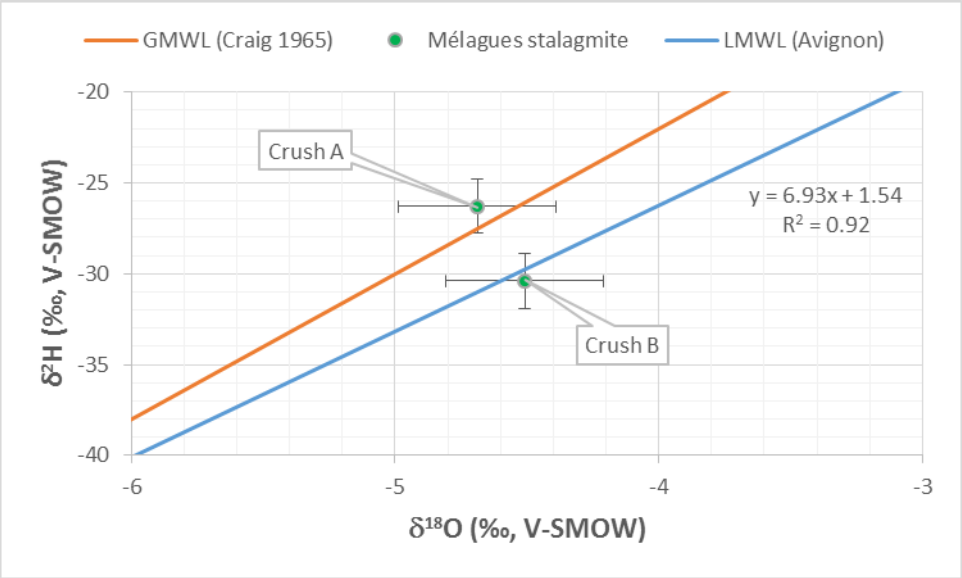

Figure 3.5. $\delta^{18}O$ and $\delta^{2}H$ values of two analysed fluid inclusion samples. The orange line represents the Global Meteoric Water Line (GMWL), while the blue line indicates the isotopic composition of present-day rainwater from Avignon: the Local Meteoric Water Line (LMWL; data from IAEA/WMO, 2013). The equation for the slope of the LMWL is also displayed, while the correlation is indicated by the R-square (n = 171). The fluid inclusion data plot on or reasonably close to both the GMWL and LMWL, taking standard deviations (<0.3‰ for $\delta^{18}O$ and <1.5‰ for $\delta^{2}H$) into consideration.

The calculated paleotemperatures from both equations, as explained in 2. Methodology, are displayed in table 3.2.

Equation	*Sample*	*Paleotemperature (°C)*
Craig (1965)	A	13.9
	B	15.8
	Average	**14.8**
Kim and O'Neil (1997)	A	12.5
	B	14.5
	Average	**13.5**

Table 3.2. Paleotemperatures of the samples, calculated using two different equations.

3.3. Colour analyses

The Matlab script shown in Appendix II was used in order to import the image, extract a colour data record from a transect along the growth axis of the stalagmite. This colour record was resampled at a 0.5 mm resolution, which resulted in 367 data points (Appendix II). Values vary among 116-255 for red, 63-236 for green and 0-163 for blue and are illustrated in figure 3.6. This intensity graph can be used to compare the colours/lamination with the isotopic composition of the speleothem. Darker colours reflect lower values, while lighter colours show higher values.

At first glance, it seems less negative carbon isotope values correlate to low peaks in the intensity of the green colour, while more negative $\delta^{18}O$ values generally seem to show higher peaks (Fig. 3.7). However, closer inspection and cross plots suggest the correlation of both isotopes with the intensity of green is insignificant in the whole record, but decreasing and slightly increasing with less negative values for carbon and oxygen, respectively (Fig. 3.8). The colour green was chosen for these analyses, because this colour is not restricted by its value, while the values for blue (cannot be lower than zero) and red (cannot be higher than 255) are.

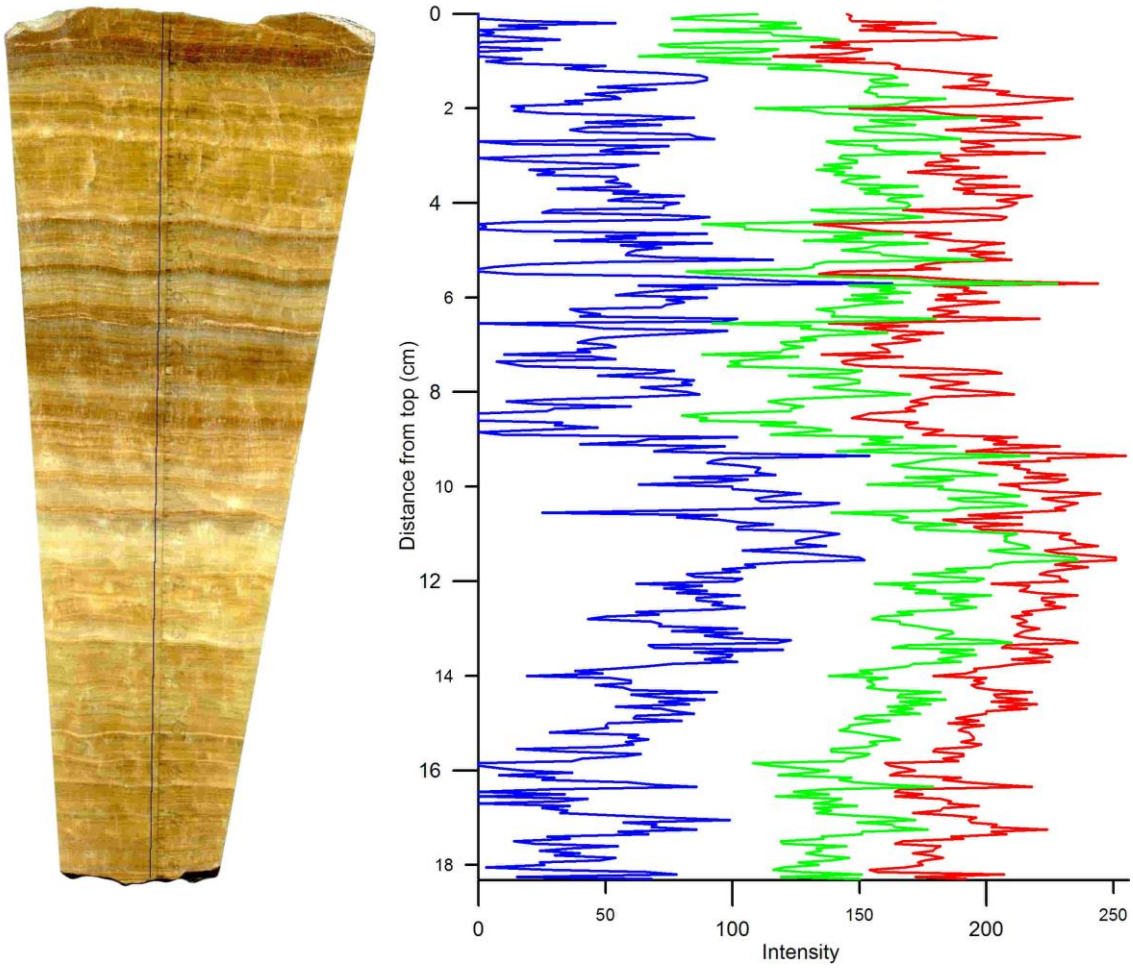

Figure 3.6. The transect of the colour analyses in Matlab along the growth axis of the stalagmite, indicated by a solid black line (left) and values for red, green and blue along the transect (right).

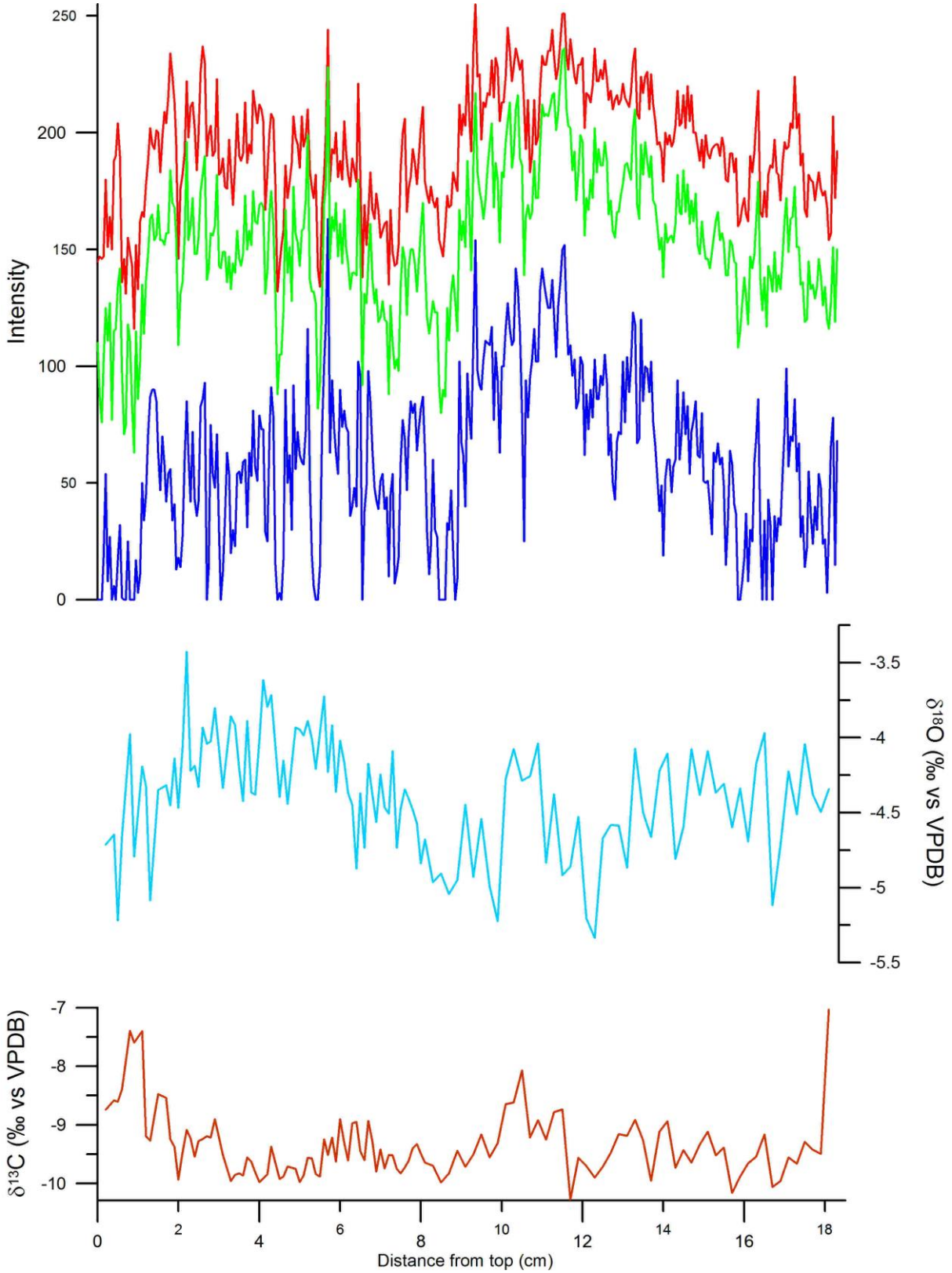

Figure 3.7. RGB data and stable isotope data ($\delta^{18}O$ in sky blue, $\delta^{13}C$ in brick red) of the Montagne Noire stalagmite.

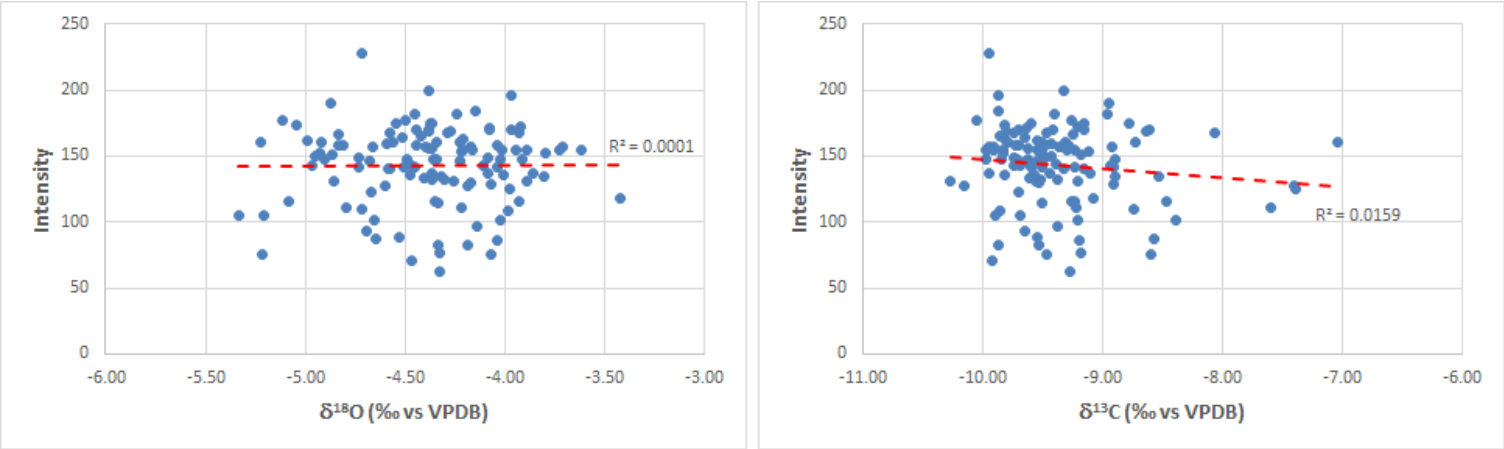

Figure 3.8. Cross plots of $\delta^{18}O$ (left) and $\delta^{13}C$ (right) with the intensity value of green in the stalagmite. The statistical fit of the linear correlation is indicated in the figure by the R-square.

3.4. Petrographic microscope analyses

Petrographic inspection showed the different growth patterns of the stalagmite. As can be inferred from figure 3.9 and figure 3.10, the speleothem shows dark layers and voids, while it also displays

(A) planar-to-crinkled layering, reflecting variable patterns of growth (parallel light),
(B) feather-shaped and fibrous-radial networks (with crossed nicols),
(C) alternating planar-to-crinkled and fibrous networks,
(D) breccia/microsparite deposits rich in Cambrian dolostone and slate clasts cemented with fibrous-radial rosettes,
(E) fibrous-radial networks with an outer rim of columnar crystals,
(F) planar-to-crinkled layering of granular calcite crystals.

For more petrographic images and the thin sections used for this analyses, see Appendix IV.

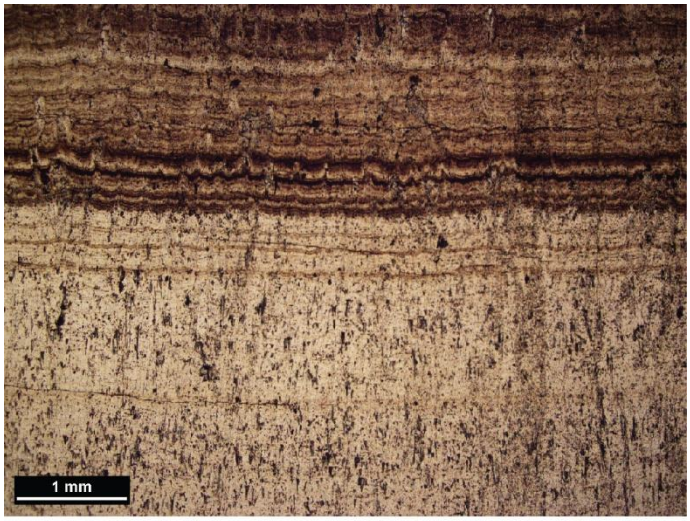

Figure 3.9. Photograph of thin section KM3, showing dark layers and voids.

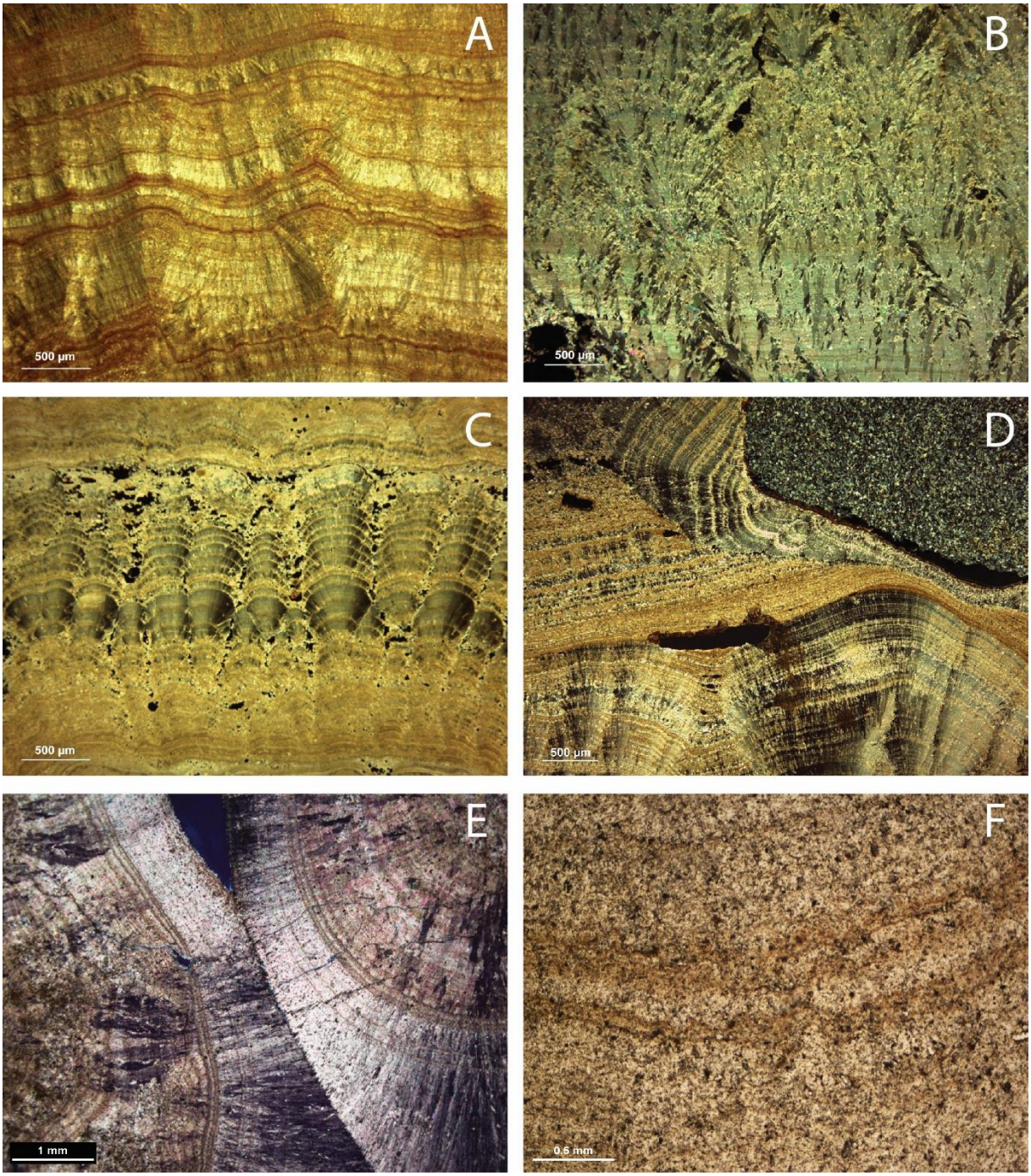

Figure 3.10. Photographs of thin sections of multiple stalagmites from the study area, showing different types of calcite crystals. A: planar-to-crinkled layering, reflecting variable patterns of growth (parallel light), B: feather-shaped and fibrous-radial networks (with crossed nicols), C: alternating planar-to-crinkled and fibrous networks, D: breccia/microsparite deposits rich in Cambrian dolostone and slate clasts cemented with fibrous-radial rosettes, E: fibrous-radial networks with an outer rim of columnar crystals, F: planar-to-crinkled layering of granular calcite crystals.

3.5. Scanning electron microscopy (SEM) and energy dispersive X-ray spectroscopy (EDS)

Both SEM and EDS analyses showed notable differences in morphology/texture and composition in the thin sections (Fig 3.11). However, the layering and fabrics from the petrographic microscope analyses are not observable at this level of detail. The colours/textures and compositions that have been distinguished are displayed in table 3.3. Apart from predominantly calcium, trace deposits of mainly iron and magnesium are also present, along with minor abundant elements of silicon, copper, aluminium, chlorine and phosphorus. However, the surface of the thin sections should have been cleaned better before the measurements were performed. Hence, these latter five elements (Si, Cu, Al, Cl and P) are ignored for the discussion, since they have low peaks and/or are considered to be contamination or dust particles on the surface of the thin sections, resulting in elevations in the SEM images and erroneous results.

See Appendix V for all scanning electron microscopy images and energy dispersive X-ray spectroscopy results.

Colour/texture	Ca	Mg	Fe	Other
White	++		+++	
Light grey	+++	+		
Dark grey	+++	++		
Black				C (+++)
Empty and partially filled voids	+++	+	+	S (+)

Table 3.3. Composition of major colours/texture changes measured in two thin sections. The pluses indicate the relative abundance of the element compared to other colours/textures after qualitative and quantitative analyses.

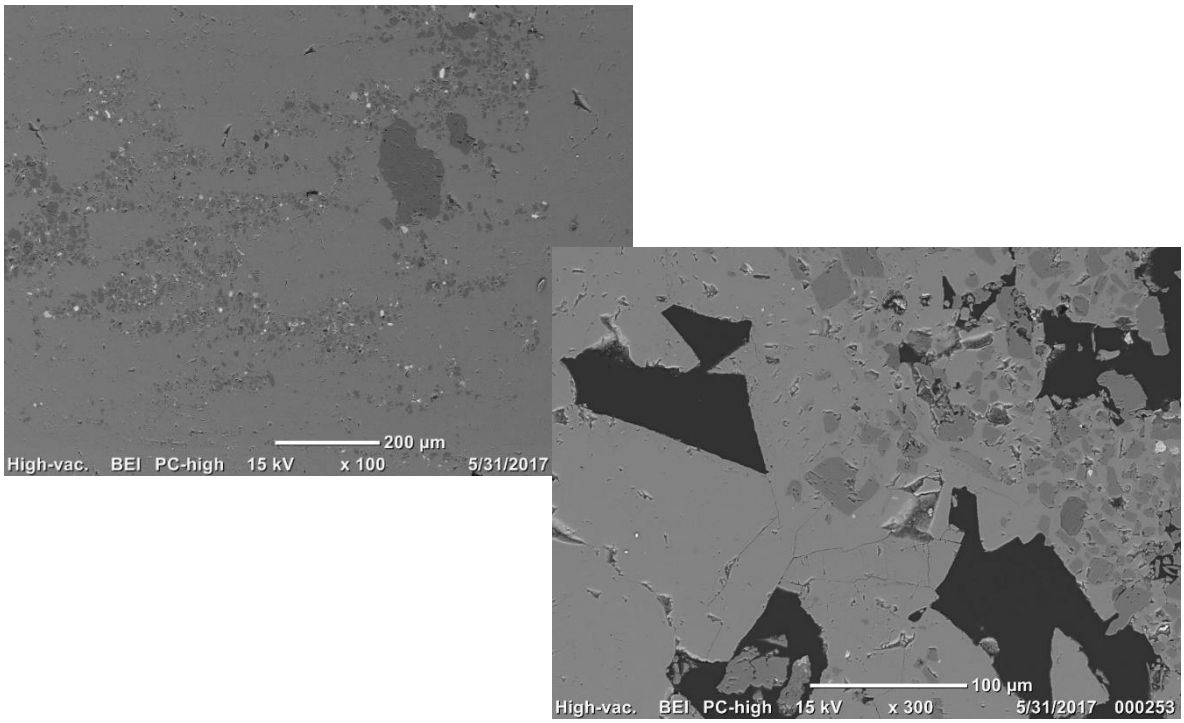

Figure 3.11. SEM images showing variations in colour (white, light grey, dark grey and black) and texture in two thin sections at different magnification levels. Composition of white colour: high Fe/moderate Ca, light grey colour: high Ca/low Mg, dark grey colour: high Ca/moderate Fe, black colour: high C, empty and partially filled void texture: high Ca/low Mg/low Fe/low S.

3.6. X-ray diffraction analyses (XRD)

Samples 1, 2 and 3 (Fig. 2.4) show a similar composition compared to each other. Most of the material (~70%) consists of magnesium calcite (major peak at ±29.5 °θ), but also evidence for less abundant dolomite (~25%, major peak at ±31 °θ) and quartz (~5%) is found.

Samples 4a, 4b and 5 show a different pattern than the first three samples, but also have a similar composition compared to each other. These analyses only show the presence of magnesium calcite, while the peaks of quartz are even smaller than in the first three samples and are, thus, negligible. For XRD analyses graphs, see Appendix VI.

4. Discussion

Nowadays, Montagne Noire in southern France is the border between two climate types. Therefore, this area is key to study climate change. To understand climate change at a broader scale and changes in precipitation in particular, a dense network of paleo-rainfall records is necessary. A low amount of speleothem proxy records in southern France strengthens the reason why a study in this area is performed.

This study provides an overview of the collected high-resolution measurements of carbon, oxygen and hydrogen isotopes and colour analyses, which contribute to the local climate reconstruction of Montagne Noire, while differences in mineralogy and crystal morphologies provide more information about the (post-)depositional characteristics of the studied stalagmite. The main aim of this research is to propose how temperature, rainfall and vegetation changed over time during the formation of the studied speleothem.

4.1. Mineralogy and crystal morphologies

4.1.1. Petrographic microscope analyses

Petrographic inspection showed the different growth patterns of the stalagmite. As can be inferred from figures 3.5 & 3.6, the speleothem shows dark layers and voids, which are interpreted to be fluid inclusion rich layers (Kendall and Broughton, 1978). It is assumed these inclusions are primary, which leads us to conclude that fluid inclusion isotope composition is undisturbed since the time of formation.

Four columnar fabrics (compact, open, elongated and spherulitic) are observable in the Montagne Noire speleothem, along with micrite, microsparite and mosaic fabrics. The four columnar types, in the given order, have ascending Mg/Ca ratios and supersaturation states (Frisia, 2015). An increase in Mg concentration in speleothems is commonly related to dry periods. As post-depositional phenomena progress, the original geochemical signal is changed. A general overview of the characteristics and environments of formation of the fabrics observed in the Montagne Noire speleothem is shown in figure 4.1.

Columnar fabrics mostly form under relatively constant discharge. In compact fabrics, a thin film of fluid is formed under relatively slow drip rate and enhanced degassing conditions, while more positive carbon isotope ratios values in the compact columnar laminae would also reflect more intense cave ventilation. Open columnar fabrics form a thicker film of fluid, under higher drip rate, less efficient degassing, discharge variability and free growth circumstances. In this study, many (fluid) inclusions are observed in the open columnar fabric. A study in the Pont-de-Ratz Cave, 35 km southeast of Mélagues, showed primary columnar calcite with dissolution voids preferentially open at the boundary between neighbouring crystals, resulting in a gradual opening of secondary voids in the primary columnar calcite (Perrin et al., 2014). Columnar elongated calcite forms under constant drip rates, similar calcite supersaturation state (SI_{cc}) but higher Mg/Ca ratios than for columnar compact and open. The last columnar type observed in the Montagne Noire speleothem, spherulitic, forms under constant flow, higher Mg/Ca ratio dripwater and SI_{cc} than those required for the development of elongated, compact or open columnar fabrics.

The presence of micrite suggests a biotic intervention by e.g., organic compounds, microbial laminae or influences of cave microbes, although $\delta^{13}C$ measurements of micrite or fluorescence analyses are necessary to confirm this. It has been suggested before that the stromatolite-like structures in speleothems mark periods of glacier retreat and reduction or cessation of the common abiotic speleothem growth processes (Frisia and Borsato, 2010; Frisia et al., 2012; Luetscher et al., 2011). It is, thus, interpreted that micrite is a result of microbial colonization of the speleothem surface during a relatively dry period with low discharge. Yet, it is unclear whether micrite fabric is a diagenetic product of destructive condensation-corrosion or a primary fabric. However, it is preferred that

aragonite needles from condensation-corrosion are replaced by microsparite than micrite. It is expected that the Montagne Noire speleothem contains both types of micrite.

Microsparite is, thus, commonly observed in association with micrite in stromatolite-like structures and in dark, organic-rich laminae within stalagmites. In the latter case, organic matter oxidation may have promoted sin-depositional dissolution-re-precipitation processes. Low-Mg calcite microsparite is inferred to be the product of aggrading neomorphism of micrite. Aggradation would occur when a flow of saturated solutions enters in contact with micrite, which should imply a partial or complete opening of the system in order for microsparite to replace micrite. Yellowish to dark brown structures in combination with fractures and (micro)sparite fabrics support this interpretation, since the cavities in the speleothem are slowly filled with (micro)sparite and organic matter and/or Fe-oxidation on the border of these dissolution voids (Fig. 3.6C-D). As aforementioned, microsparite is also typical as a replacement phase in aragonite needles in the form of mosaics of calcite crystals. All three discussed types are observed in the studied speleothem. Thus, it is proposed that occurrence of microsparite fabric in speleothems is indicative of diagenetic processes and/or facilitated by the presence of organic compounds.

If this diagenesis continues, mosaic-like structures can form, which are, in the Montagne Noire speleothem, most probably a product of dissolution of columnar calcite and re-precipitation of mosaic calcite driven by influx of undersaturated waters causing dissolution of a pre-existing fabric, and re-precipitation of sub-euhedral crystals. However, mosaic calcite can also be the final product of neomorphism in a micrite → microsparite → sparite series (Frisia, 2015).

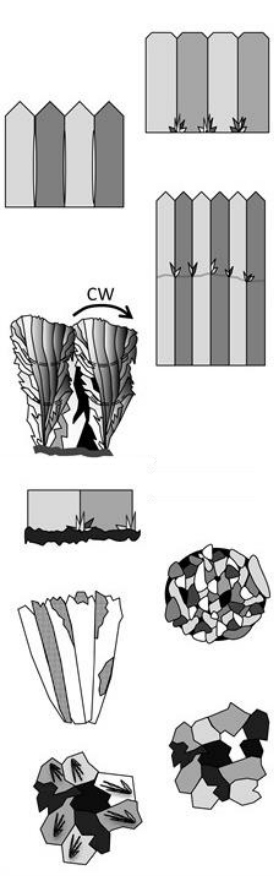

Type	Characteristics	Environment of formation
Columnar	l/w ratio <6:1; competitive growth at interfaces; straight to serrated boundaries; uniform extinction; common "flat" terminations or protruding rhombohedra terminations (~ 2µm high)	Relatively slow and constant drip; Slcc < 0.35; Mg/Ca <0.3; pH up to 8. 4; low impurity content
Columnar open	l/w ratio <6:1; competitive growth at interfaces; incomplete coalescence of crystals; high intercrystalline porosity, commonly linear; uniform extinction.	Drip rate > than in C; Slcc up to 0.35; Mg/Ca <<0.3; pH 7.5 up to 8.
Columnar elongated	l/w ratio > 6:1; competitive growth at interfaces; preferential growth of acute rhombohedron; incomplete coalescence of crystals; protruding terminations common; uniform extinction. May show lateral overgrowths, in particular in the presence of impurity-rich layers.	Drip rate constant; Slcc 0.1 to 0.4; Mg/Ca > 0.3.
Columnar radiaxial	Polycrystals l/w ratio > 6:1; undulatory extinction converge away from substrate when rotating table turned CW; split crystal growth; upward concave curvature.	Low drip rate or laminar flow; Slcc 0.5; Mg/Ca > 1.5; typical in stalagmites & flowstones formed in caves cut in dolomite
Micrite	Crystals < 2µm; stromatolitic-like structure; clotted structure. Common geometric selection above micrite layers.	Bio-influenced. Low flow/dry. Condensation/corrosion?
Microsparite	l/w ratio ~ 1:1; crystal size > 2µm < 30µm; commonly associated with micrite. Fabric-destructive replacement.	Diagenesis. Aggrading neomorphism (micrite to microsparite)
Replacive microsparite	l/w ratio ~ 1:1; Crystal size > 2µm < 30µm; retention of aragonite fabric.	Diagenesis. Mimetic replacement
Mosaic calcite	l/w ratio ~ 1:1; crystal size > 30µm. Fabric destructive.	Diagenesis. If replacing calcite, no relicts of a former unstable phase are visible.
Mosaic calcite with aragonite needles	l/w ratio ~ 1:1; Crystal size > 30µm; Fabric destructive; preserves relicts of aragonite, commonly needles.	Diagenesis. Commonly related to the transformation of speleothem aragonite into calcite

Figure 4.1. Indication of the characteristics and environments of formation of the fabrics observed in the Montagne Noire speleothem. Modified after Frisia (2015).

4.1.2. SEM & EDS

Both scanning electron microscope imaging and energy dispersive X-ray spectroscopy analyses showed notable differences in morphology/texture and composition in the thin sections. However, the layering and fabrics from the petrographic microscope analyses are not observable at this level of detail. All colours and dissolution structures are rich in calcium, except for black textures, which mainly show high carbon peaks. Light grey is assumed to be the matrix colour.

Analyses 2c and 2.1d (Appendix V) are most representative for the matrix, since the light grey colour is composed of calcium carbonate with a low magnesium content. Partially filled voids show the same composition as the matrix, with a slightly higher content of Fe and/or S. This indicates the presence of organic matter. Darker grey colours show higher Mg concentrations and more fractures, possibly filled with microorganisms. Unfortunately, since our equipment is a desktop SEM, it was not able to zoom in sufficiently enough in order to confirm this.

White parts in the thin sections showed similarities with the Fe-rich minerals siderite, ankerite and/or Fe-rich dolomite. These iron-rich clay minerals in the studied speleothem suggest diagenetic processes and/or siliciclastic input after deposition of the carbonate, possibly linked to percolating water through the host-rock dolomite. Deposits rich in iron or sulphur and organic matter are often found together and may thus also be related to reducing (anoxic) conditions.

The origin of the black colour is unclear at this time. It is reasonable to assume the colour is explained by the carbon coating that has been applied to the thin sections and then measured, since a clear gap in the thin section is observed. Additionally, the gap does not show any evidences for microbial activity.

4.1.3. XRD

When combining the SEM and EDS data with the results of the XRD analyses, it becomes clear the stalagmite is indeed mainly composed of magnesium calcite. Local white spots in the stalagmite seem to be different from the rest of the speleothem and are thought to contain higher concentrations of iron, which are represented by major and secondary peaks that are typical for iron-rich dolomite. The XRD analyses, thus, lend further support for the interpretation that some elements of the original material were replaced by iron through diagenetic processes. Furthermore, there is evidence to rule out the aforementioned Fe-rich minerals siderite and ankerite from the EDS analyses, since only iron-rich dolomite is observed in the XRD analyses.

In summary, this stalagmite is a magnesium calcite with local iron-rich traces of dolomite. Weathering and (under)groundwater caused dissolution and precipitation of the magnesium calcite. Due to diagenesis, dolomitization and/or inputs of siliciclastic/host-rock material, parts of the stalagmite became enriched in Fe-rich dolomite. Partial dissolution (~5%) of the speleothem led to small voids (<40 µm) that were subsequently (partially) refilled by bacteria and microorganisms. The presence of iron and organic matter suggests some local reducing conditions. Since post-depositional processes altered the original geochemical composition of the stalagmite only to some extent, it is still useful to measure stable isotopes for paleoclimate research.

4.2. Climate interpretation: stable isotopes

4.2.1. Carbon isotopes

The $\delta^{13}C$ values of the Montagne Noire stalagmite range between -10.27 and -7.04‰ VPDB. No large shifts in $\delta^{13}C$ occur, except perhaps for the bottom of the stalagmite, which displays the highest $\delta^{13}C$ values.

These $\delta^{13}C$ values are typical for speleothems formed in equilibrium with CO_2 respired from C3 plants (McDermott, 2004), which nowadays occur in the temperate region of our study area (Inventaire Forestier National, 1995). Higher $\delta^{13}C$ values can usually be attributed to closed cave systems, but in practice most natural systems are partially open (McDermott, 2004). The relatively low $\delta^{13}C$ values in the Montagne Noire stalagmite might be explained by periods of climatic amelioration, leading to a progression in the production of soil biogenic CO_2, which is interpreted based on a stalagmite from Villars, 260 km northwest of Mélagues (Genty et al., 2003). Since soil activity and prior calcite precipitation (PCP; carbonate precipitation from infiltrating water before the water drips on a stalagmite) are closely related to each other, more negative $\delta^{13}C$ values might reflect decreased PCP during warmer (and wetter) periods, certainly on a seasonal time scale (Van Rampelbergh et al., 2015).

An increase in precipitation amount might also cause a decrease in the $\delta^{13}C$ value of speleothem calcite by increasing soil moisture content and soil respiration rates or by reducing water-rock interactions, thereby reducing the amount of $\delta^{13}C$-enriched carbon derived from the host limestone (Van Breukelen, 2009).

Alternative explanations for the low carbon isotope values in the studied stalagmite include: low amounts of evaporation, slow degassing of cave drip-waters, long residence times, little degassing of CO_2 and little calcite precipitation in the vadose zone above the cave (McDermott, 2004). It is not likely the altitude effect can explain the low $\delta^{13}C$ values, since a relatively low altitude would then be expected (Johnston et al., 2013), which is not the case in our study area.

4.2.2. Oxygen isotopes

The Montagne Noire stalagmite shows a variation in oxygen isotope values between -5.34 and -3.43‰ VPDB, which is relatively high compared to other European records (Boch et al., 2011; Boch et al., 2009; Frisia et al., 2002; Frisia et al., 2007; Fuller et al., 2008; Lauritzen and Lundberg, 1999; Miorandi et al., 2007; Plagnes et al., 2002; Riechelmann, 2010; Riechelmann et al., 2011; Sundqvist et al., 2007). Larger shifts in $\delta^{18}O$ seem to occur towards the bottom of the stalagmite. The modern-day average annual oxygen isotope composition in precipitation around the study site is lower than in the Montagne Noire stalagmite (-5.70 ± 1.14‰ V-SMOW; IAEA/WMO, 2013).

In order to correctly interpret the oxygen isotope signal in terms of fractionation, it is necessary to assume the studied stalagmite has formed under oxygen isotopic equilibrium, since kinetic fractionation in speleothems deposited at disequilibrium results in isotope covariations (Hendy, 1971). Speleothems form at oxygen isotopic equilibrium with drip waters if the mode of deposition was by relatively slow outgassing of CO_2 from the drip water. This occurs in caves where relative humidity was ~100% and where lack of significant movement of air resulted in high partial pressure of CO_2, resulting in a slow outgassing of drip water (Schwarcz, 2007). No so-called Hendy tests have been performed to confirm these equilibrium conditions during growth. However, if the cave air temperature is close to the mean annual air temperature above the cave, changes in cave temperature and therefore changes in fractionation have a direct link with regional climatic parameters (Verheyden et al., 2014). Since the cave formed close to the surface, the seasonal cave temperature variations are likely to be smaller than 1 °C (Wigley and Brown, 1976), suggesting that the seasonal $\delta^{18}O$ signal in the speleothem is mainly controlled by the $\delta^{18}O$ composition of the cave seepage water (Van Breukelen, 2009). This implies that large-scale fractionation in the Montagne Noire speleothem is unlikely, while also the narrow range of both isotopes measured in the stalagmite supports this interpretation.

The oxygen isotope composition in speleothems is influenced by several factors; major factors like the oxygen isotope composition of cave drip water and precipitation, the temperature at which the precipitation occurs and changes in amount effect, but also minor factors, such as changes in moisture source or transport pathways, the altitude, orographic and continental/rainout effects (Blisniuk and Stern, 2005; Dansgaard, 1964; Johnston et al., 2013; McDermott et al., 2011; Van Breukelen, 2009; Verheyden, 2001; Verheyden et al., 2014).

The average $\delta^{18}O$ value (-4.38‰) measured in the Montagne Noire stalagmite can, thus, be interpreted as relatively low precipitation amounts in dry periods. Shifts to lower $\delta^{18}O$ values therefore indicate pulses of relatively wetter conditions, assuming the annual cave temperature remains constant (Verheyden, 2001). Higher oxygen isotope values also would be expected on the wet windward side of the barrier (orographic effect) and close to the moisture source (continental/rainout effect; Blisniuk and Stern, 2005; Lachniet, 2009). The study area is relatively far (> 350 km) from its oceanic source and on the windward side of the mountain, since the dominant wind direction is west to southwest in the Montagne Noire region (Inventaire Forestier National, 1995). Interpretations based on the oxygen isotope composition of precipitation or amount, orographic and continental effects, hence, contradict each other. A change of transport pathways and dominant wind direction could possibly give an explanation for this contradiction, but the general Atlantic moisture circulation pattern does not seem to have changed on a multi-decadal timescale during the Holocene (McDermott et al., 2011).

However, when considering precipitation is also from Mediterranean origin, mainly during summer and fall, the relatively high oxygen isotopes values can be further explained. First of all, rainfall in July shows a significantly higher $\delta^{18}O$ value (-2.40‰ V-SMOW) compared to other months (minimum of -7.60‰ V-SMOW in February around Avignon; IAEA/WMO, 2013). Although the present-day summer precipitation is low (∼100 mm in total in June, July and August vs. ∼550 mm in the rest of the year around Avignon; IAEA/WMO, 2013) and the area is dry, it is sufficient enough to form speleothems in this region. This means that during violent storms during summer, fall or even spring, the southern winds blow towards Montagne Noire and causes more positive $\delta^{18}O$ to precipitate relatively close to its moisture source. Nowadays, this cold Mediterranean air is felt up to Millau and Camarès, which are situated more towards the lee side of the barrier (seen from the Mediterranean Sea; Inventaire Forestier National, 1995). These same processes could have occurred during the formation of the studied speleothem as well, indicating seasonal Mediterranean precipitation is dominating our $\delta^{18}O$ record. This is an essential explanation for the relatively high $\delta^{18}O$ values measured in the Montagne Noire stalagmite, since it is in good agreement with the higher values of rain and sea water around our study site predicted in oxygen isotope simulation studies (Lachniet, 2009; LeGrande and Schmidt, 2006). Mediterranean influences thus result in locally higher $\delta^{18}O$ values of precipitation, since the Mediterranean Sea is isotopically heavier than the Atlantic Ocean due to high evaporation rates from the relatively small water basin compared to the Atlantic Ocean (Lachniet, 2009). Studies from other nearby cave sites confirm the oxygen isotope compositions of cave seepage water and a speleothem are relatively heavier in the studied region compared to other European caves (Plagnes et al., 2002; Wackerbarth et al., 2012).

The Mediterranean effect only influences oxygen isotopes (mainly during relatively dry summers), which possibly explains why there is no relationship between $\delta^{18}O$ and $\delta^{13}C$ values ($R^2 \approx 0.0055$) and why our oxygen isotope interpretation is in contradiction with our carbon isotope interpretation, in which we suggest the isotopically light $\delta^{13}C$ values can be explained by relatively warm and wet periods.

Since this study is one of first in the region of Montagne Noire as far as we know and little work has explored the spatial variations in $\delta^{18}O_{ct}$, it is currently not possible to give an explanation for the altitude effect. However, a decrease in the mean oxygen isotope values of cave dripwater and speleothems should be expected with an increase in altitude within the region (Johnston et al., 2013;

Lachniet, 2009). Based on two caves from Italy located around the same altitude as our study site, it was expected the $\delta^{18}O_{ct}$ values would have been 2 to 4‰ lower (Johnston et al., 2013). Although the moisture source is also the Mediterranean Sea, the progressive rainout effect is of major influence for the two Italian caves, since air masses encounter multiple high (>1500 m) barriers before reaching the area of these caves. Significantly lower oxygen isotope values compared to our study site are therefore found in the valleys where the Italian caves are located. In addition, calculated paleotemperatures resulting from 2 to 4‰ lower $\delta^{18}O_{ct}$ values show unlikely climate conditions (22-31 °C) during deposition, which makes our comparison of altitude effects criticisable.

Generally, our interpretation is good agreement with the interpretation of Wackerbarth et al. (2012), who modelled the $\delta^{18}O_{ct}$ values in European caves. Their model is based on multiple measured $\delta^{18}O_{ct}$ and $\delta^{18}O_{rainfall}$ values throughout Europe including one of the Clamouse Cave. The model showed an increase in $\delta^{18}O_{ct}$ values in southern France and other parts around the Mediterranean Sea as the consequence of increases in temperature and the oxygen isotope composition of rainfall, along with a decrease in precipitation (Wackerbarth et al., 2012).

4.2.3. Hydrogen isotopes and fluid inclusions

Results from the Amsterdam Device 1.0 show ~4.11‰ variation in $\delta^{2}H$ values and ~0.18‰ (V-SMOW) in $\delta^{18}O$ values after corrections. The water yields from both analyses are remarkably low (<0.1 µl) compared to fluid inclusions in other speleothems (De Bie, 2017; Van Breukelen, 2009), with the youngest sample displaying the lowest amount of water. The average annual hydrogen isotope composition in the precipitation around our study site is much lower than the $\delta^{2}H$ values observed in the Montagne Noire speleothem (-38.12 ± 7.89‰ in Avignon vs. -28.34‰ V-SMOW in the studied speleothem; IAEA/WMO, 2013).

Often, $\delta^{2}H$ and $\delta^{18}O$ data plot near the GMWL, which lends support to the accuracy of the analyses (Vonhof et al., 2007). The Montagne Noire speleothem $\delta^{18}O/\delta^{2}H$ data plots reasonably close to the GMWL, indicating that these values are accurate. The present-day rainwater isotope data for Avignon generally plots on the GMWL, which provides further support for a good preservation of the original isotope composition of fluid inclusion water in the studied speleothem, since post-depositional changes in the fluid inclusion water isotope composition would have driven the water away from the GMWL (Van Breukelen et al., 2008).

It has been established that cave drip water, and thus fluid inclusion water, is isotopically identical to local rainwater for $\delta^{2}H$ and $\delta^{18}O$ (Van Breukelen, 2009). By analysing these fluid inclusions, it is possible to provide the $\delta^{18}O$ value of drip water through time, which is usually the most important unknown in paleotemperature equations. The equation most relevant for this study is the one by Kim and O'Neil (1997), since the Montagne Noire speleothem has a calcite mineralogy. In order to compare the differences in paleotemperature equations, also the formula by Craig (1965), based on mixed marine calcite and aragonite, is used. The latter equation generally gives the more accurate results, since the Kim and O'Neil (1997) equation leads to temperatures that are several °C too low (McDermott et al., 2006).

Application of the Craig (1965) equation to the Montagne Noire record results in an average paleotemperature of ~14.8 °C, indeed much closer to the modern annual average temperature in Avignon of 14.8 ± 0.9 °C than the ~13.5 °C calculated from the Kim and O'Neil (1997) equation. Although only two measurements were made of the speleothem, which makes our interpretation less accurate, a decreasing trend in temperature is observed towards the top of the stalagmite.

4.3. Climate interpretation: colour analyses

The colour records confirm that darker layers with lower values for red, green and blue are present at the top half of the stalagmite, while the intensities of these colours are higher in the bottom half. There is no correlation between the RGB values and the stable isotopes, although the correlation with $\delta^{13}C$ is less insignificant. The precise controls on the relation between the colours and geochemical composition in speleothems are poorly understood, but a few suggestions are proposed here.

Dry periods should show, next to relatively more positive $\delta^{18}O$ and $\delta^{13}C$ values, darker and more densely packed lamination in the speleothem (Van Rampelbergh et al., 2015). The density of the layers in the Montagne Noire stalagmite does not differ much, but it seems darker laminae on the top half of the stalagmite rather show thinner layers than thicker ones. This seems consistent with the interpretation of Van Rampelbergh et al. (2015), except the presence of the reddish-brown iron-rich layers suggests wetter periods due to higher concentrations of organic matter, while colourless calcite deposits form in drier periods (Asrat et al., 2008; Baker et al., 2007; Baker et al., 2008). However, oxygen and carbon isotope measurements of the speleothems used in these aforementioned studies possibly indicate non-equilibrium conditions during deposition, which makes the interpretation less trustworthy.

Additionally, rapid fluctuations in $\delta^{18}O$ are present, while oxygen isotope values are higher in the top darker part of the Montagne Noire stalagmite compared to the colourless area towards the bottom. Carbon isotope values seems to rise more consistently in brown laminae (and thus indicate wetter conditions). A clear interpretation for the variations in calcite colour in this speleothem is, thus, not present at this time, but it is reasonable to assume colourless layers formed during relatively dry periods and reddish-brown laminae during relatively wet periods.

4.4. Comparing Montagne Noire with other regions

4.4.1. Scladina (Belgium)

At the same time of this project, a comparable research has been performed on speleothems from the Scladina Cave, Belgium (De Bie, 2017). The Scladina Cave (50.5°N, 5.0°E) is situated in the village of Sclayn (Andennes, Namur, Belgium) at the southern bank of the Meuse River. Multiple paleoclimate studies have been performed in this cave, also due to its high archaeological value. The collected data from the French and Belgian stalagmites will be discussed and compared with each other in order to gain more information about the possible age of the Montagne Noire record and climatic conditions during deposition of the stalagmites.

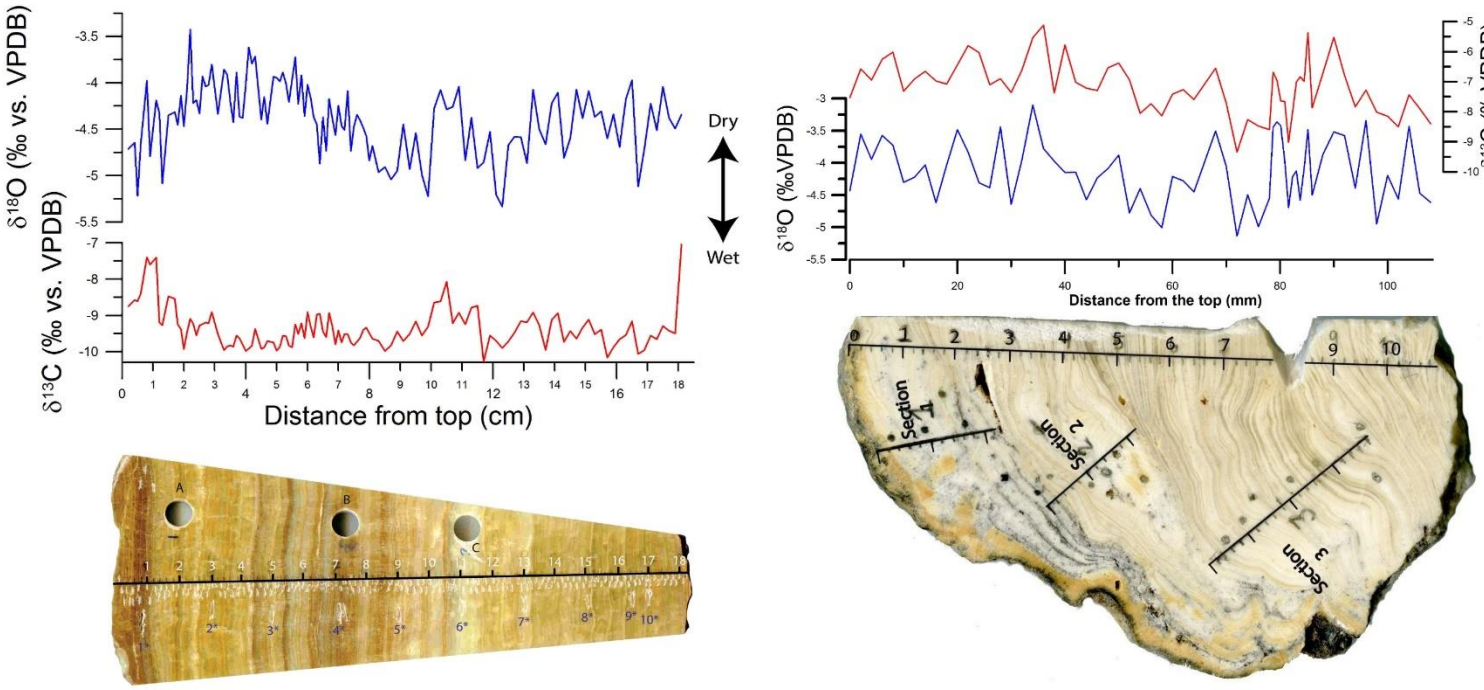

Figure 4.2. The Montagne Noire (left) and Scladina (right) stalagmite with their $\delta^{18}O$ and $\delta^{13}C$ values visualized in diagrams. See Appendix III for more detailed graphs of both stalagmites.

The first striking difference between the two stalagmites is the colour of their layers. The layers in the Scladina stalagmite consist of an alternation between beige-white transparent and milky white layers with black and yellowish layers at the edge, due to post-depositional changes, while the Montagne Noire stalagmite has dark brown layers at the top, which gradually become lighter until a depth of ± 90 mm. The colour gets darker again beyond ± 120 mm. The more defined colours of the French stalagmite can be an indication for better preservation compared to the Scladina stalagmite, but the colour differences between the two speleothems also might have been caused by differences in the overlying bedrock from which the stalagmites have formed (dolomite in France and limestone in Belgium). It is thought the Montagne Noire stalagmite has a higher concentration of humid substances in its darker layers, while the milky white laminae along the growth axis of the Scladina stalagmite do not show such phenomena.

The $\delta^{13}C$ values of the Montagne Noire stalagmite are relatively low and range between -10.27 and -7.04‰, while the carbon isotope values of the Scladina MIS 7 stalagmite range between -9.35 and -3.20‰ (Fig. 4.2). Compared to the stalagmite from France, the $\delta^{13}C$ values of the Scladina stalagmite differ much more along its longitudinal growth axis.

The oxygen isotope values of the French stalagmite range between -5.34 and -3.43‰ and the $\delta^{18}O$ values of the Scladina stalagmite between -5.14 and -2.75‰ (Fig. 4.2). Thus, the oxygen isotope composition of both stalagmites are very similar, unlike the $\delta^{13}C$ values. Additionally, relatively low carbon isotope values suggest more precipitation, while these wetter conditions are associated with lower $\delta^{18}O$ values.

The difference in carbon isotope values but similar $\delta^{18}O$ signal in the Scladina and Montagne Noire stalagmites can be explained by the seasonal Mediterranean source of rainfall in the region. This Mediterranean impact results in higher oxygen isotope values in the source water, since the Mediterranean Sea is isotopically heavier due to higher evaporation rates compared to the Atlantic Ocean (Lachniet, 2009), which is the origin of moisture in the study region of the Scladina stalagmite. It seems that the Montagne Noire stalagmite is a more seasonally biased-record than the Scladina one.

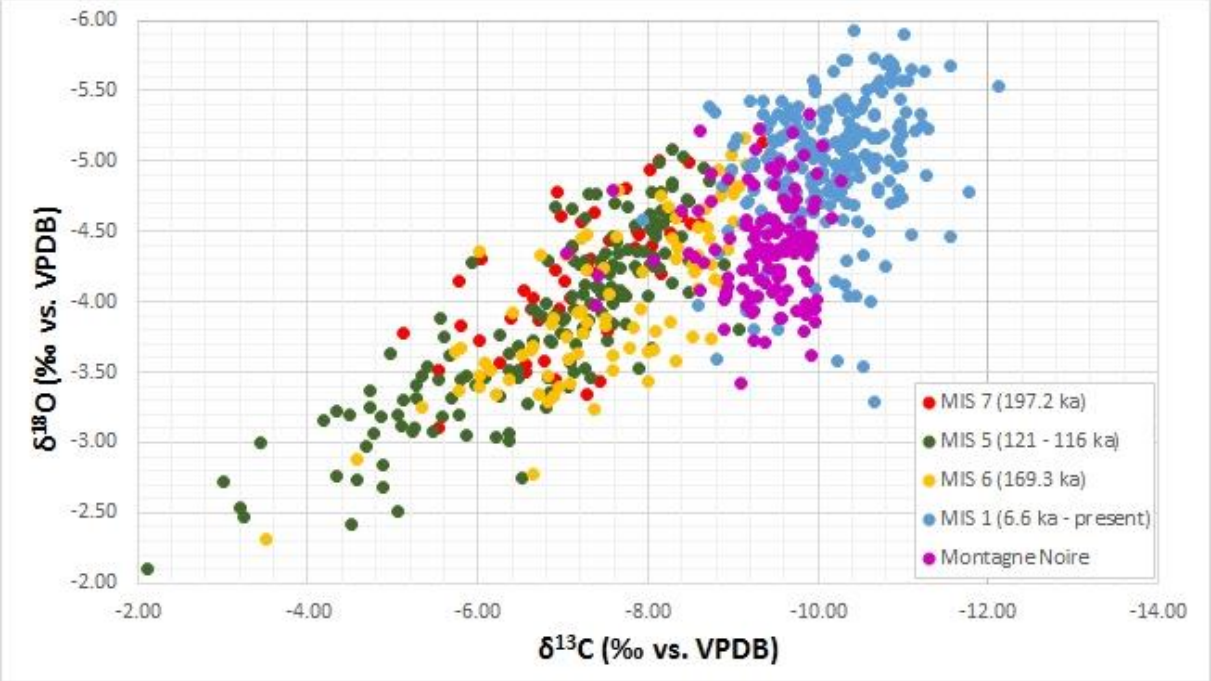

Figure 4.3. Cross plot of the $\delta^{18}O$ and $\delta^{13}C$ values of the CC6 (MIS 6), CC4 (MIS 5), CC1 (Holocene/MIS 1; Van Nunen, 2011) stalagmites and the Scladina stalagmite used in the study of De Bie (2017; MIS 7) compared to the Montagne Noire stalagmite.

The relatively little variation in the oxygen and carbon isotope values of the French stalagmite compared to the larger variation in the $\delta^{18}O$ and $\delta^{13}C$ values of the Belgian stalagmite implies that conditions during the deposition of the stalagmite from France were more stable in comparison with the conditions during the deposition of the Scladina stalagmite. Another possible explanation is that the France stalagmite contains less time in its record. However, this is unlikely, since the average growth rate of stalagmites is generally high (50-100 µm/year) and the length of the French speleothem is almost twice the length of the Scladina stalagmite: 18 vs. 10.8 cm, respectively.

The cross plot (Fig. 4.3) shows a cluster at relatively low $\delta^{13}C$ values from the Montagne Noire stalagmite, while the $\delta^{13}C$ values of the Scladina (MIS 7) stalagmite are more spread out and relatively higher than those of the stalagmite from France. The lower $\delta^{13}C$ values of the Montagne Noire stalagmite compared to the Scladina MIS 5, MIS 6 and MIS 7 stalagmites indicate more soil activity (dense vegetation cover) and less intense PCP and thus wetter conditions during the formation of the French speleothem.

The oxygen and carbon isotope values of the Belgian CC1 (Holocene/MIS 1) stalagmite shows a similar cluster compared to the $\delta^{18}O$ and $\delta^{13}C$ cluster of the French stalagmite. These resemblance implies comparable climatic conditions during the deposition of the Montagne Noire and Holocene stalagmite, which can be an indication for the possible age of the Montagne Noire stalagmite. Higher $\delta^{18}O$ values in the French record compared to the CC1 Scladina stalagmite can be explained by the previously described influences of Mediterranean derived rainfall.

4.4.2. France

Other paleoenvironmental studies from around southern France, which investigated stable isotope compositions in speleothems from different time periods, are in good agreement with our results (McDermott et al., 1999; Plagnes et al., 2002). Remarkable is that all three studies, including this one, show generally more positive $\delta^{18}O$ values. Based on the isotope values of modern active calcite deposits in the Clamouse Cave (Plagnes et al., 2002), it is reasonable to assume there are some similarities in environmental conditions, but the present-day climate is not completely the same as during the forming of the Montagne Noire stalagmite (Fig 4.4).

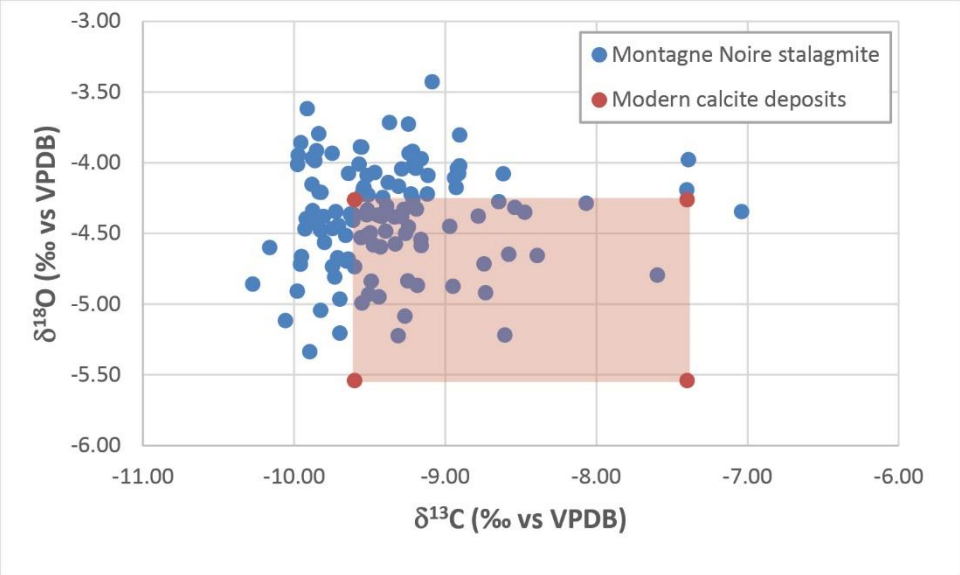

Figure 4.4. Cross plotted are the stable isotopes $\delta^{18}O$ and $\delta^{13}C$ of the Montagne Noire stalagmite (blue dots) and the range of modern active calcite deposits in the Clamouse Cave (red box; Plagnes et al., 2002).

The Mediterranean influence is also registered close to the Atlantic Ocean in the Villars Cave (Genty et al., 2003). Nevertheless, a timeframe for the Montagne Noire speleothem is necessary in order to discuss more relevant comparisons between the studies other than discussed in this chapter.

4.5. Comparing Montagne Noire with natural variabilities and climate oscillations

The stable isotope data and a REDFIT spectral analyses show small amplitudes (<1.3‰ for $\delta^{18}O$ and <1.9‰ and one of 2.5‰ for $\delta^{13}C$) at relatively small-scale intervals (<5 mm and one of 120 mm).

Unfortunately, the studied speleothem has not been dated in this project, so it becomes hard to indicate what climate oscillations these cycles exactly represent. However, it might be possible to interpret the Montagne Noire record using the growth rate of the stalagmite. During constant growth of the speleothem, which is unlikely in times of extremely cold and dry conditions, the average growth rate in other speleothems, including a few from the Clamouse Cave, is generally between 50-100 µm per year (Kaufmann and Dreybrodt, 2004; McMillan et al., 2005; Partin et al., 2008; Plagnes et al., 2002). This suggests the Montagne Noire speleothem is at least 1800 years old, so the small-scale intervals in our record probably reflect (multi)decadal oscillations, while the single larger cycle could also reflect multi-centennial up to millennial time-scale oscillations. In that case however, larger amplitudes in at least the oxygen isotope composition would have been expected. Yet again, dating of the studied stalagmite needs to be performed in order to confirm these hypotheses.

5. Conclusions

The speleothem used in this study, mainly composed of a magnesium calcite, is dominated by seasonal Mediterranean precipitation and mainly formed during relatively dry and warm periods. The vegetation during the deposition of the stalagmite is similar to the present trees and plants observed in the study area. Differences in cave conditions during and after deposition are observed through differences in mineralogy and crystal morphologies. Dating of the studied stalagmite needs to be performed in order to confirm hypotheses regarding comparisons with other regions and climate oscillations.

1. The carbon isotope signal in the studied stalagmite indicates the speleothem formed in a partially open cave and in equilibrium with CO_2 respired from **C3 plants**, the same as modern-day vegetation. Although the $\delta^{13}C$ values are relatively stable, lower carbon isotope values in the Montagne Noire stalagmite can be explained by multiple causes, such as increased precipitation, increased production of soil biogenic CO_2 or low amounts of evaporation. The few higher carbon isotope values suggest short pulses of relatively drier conditions.
2. The relatively high average $\delta^{18}O$ value, in combination with low water yields in fluid inclusions, indicate the speleothem has formed under ***relatively* dry conditions**, but still wet enough for calcite to be precipitated. Shifts to lighter oxygen isotope values indicate pulses of relatively wetter conditions, assuming the annual cave temperature remains constant. In addition, it is proposed the $\delta^{18}O$ signal is dominated by seasonal Mediterranean precipitation. Thus, the increase in oxygen isotope values in the Montagne Noire record is a consequence of increases in temperature and $\delta^{18}O$ composition of precipitation, along with a decrease in precipitation. The Mediterranean effect only influences oxygen isotopes, which possibly explains why there is no relationship between $\delta^{18}O$ and $\delta^{13}C$ values.
3. Presently, the non-existent correlation between isotope values and RGB intensity, the presence of reddish brown iron-rich laminae and the interpretation based on the visual appearance do not lead to a clear interpretation for the variations in calcite colours in the speleothem. However, it is reasonable to assume **colourless layers formed during relatively dry periods and reddish-brown laminae during relatively wet periods**.
4. Fluid inclusion analyses confirm that the Montagne Noire speleothem was formed under remarkably dry and relatively warm conditions. Our $\delta^{18}O$ data does not plot away from the Global Meteoric Water Line, indicating the data used for our interpretation is accurate. Application of the Craig (1965) equation to the Montagne Noire record results in an **average paleotemperature of ~14.8 °C**, which is similar to the modern annual average temperature in Avignon of 14.8 ± 0.9 °C.
5. Petrographic microscope analyses showed the presence of **four columnar fabrics** (compact, open, elongated and spherulitic). It is proposed that these types, in the given order, show ascending Mg/Ca ratios and supersaturation rates, which in turn are related to increasingly drier periods.

   Micrite observed the Montagne Noire stalagmite suggest microbial colonization of the speleothem surface during a relatively dry period with low discharge. As soon as the diagenesis of the rock continues, **(micro)sparite and mosaic-like structures** can form. Microsparite can replace micrite via aggrading neomorphism, which would occur when the cave system partially or completely opened. The mosaic fabric in the speleothem is probably a product of dissolution of columnar calcite and re-precipitation of mosaic calcite, but can also be the final product of the neomorphism discussed above.
6. Mineralogical (XRD) and microscopic (SEM & EDS) analyses showed notable differences in morphology/texture and composition in the thin sections. The studied stalagmite is a **magnesium calcite with local iron-rich traces of dolomite**. Weathering and (under)groundwater caused dissolution and precipitation of the magnesium calcite. Due to diagenesis, dolomitization and/or

inputs of siliciclastic/host-rock material, parts of the stalagmite became enriched in Fe-rich dolomite. Partial dissolution (~5%) of the speleothem led to small voids (<40 µm) that were subsequently (partially) refilled by bacteria and microorganisms. The presence of iron and organic matter suggests some local reducing conditions.

7. The isotope values of the Montagne Noire stalagmite are similar to a Holocene stalagmite from Scladina (Belgium), which can be an indication for the possible age of the speleothem used in this study. Isotope values of modern active calcite deposits in the Clamouse Cave (France) imply it is reasonable to assume there are some similarities in environmental conditions between the present-day climate and the climate during deposition of the Montagne Noire stalagmite.
8. Since the studied speleothem has not been dated, it is hard to indicate what the observed cycles in isotope values represent. Based on the average growth rate of stalagmites, the small-scale intervals in the Montagne Noire record probably reflect (multi)decadal oscillations, while the single larger cycle could also reflect multi-centennial up to millennial time-scale oscillations. In that case however, larger amplitudes in at least the oxygen isotope composition would have been expected.

6. Recommendations

As aforementioned, one or more datings (e.g., U/Th) have to be performed on the Montagne Noire stalagmite in order to elaborate on the time of deposition. Additionally, trace element measurements could lend support to our interpretations and at least give a better insight in both cave and climate conditions during deposition. More SEM imaging, EDS, fluid inclusion and stable isotope analyses, especially from other parts of the Mélagues speleothems, are always good to have and will certainly improve the reliability of this study. Fluorescence (UV) analyses in the observed micrite fabric might confirm the presence of organic compounds in the studied stalagmite.

On a larger scale, more speleothem records from southern France are needed in order to develop a better understanding of the climate in the past in and around our study area. Finally, other speleothem records on the lee and windward side of Montagne Noire can possibly contribute to an explanation of the altitude effect.

Acknowledgements

I would like to thank Mónica Sanchez-Román and Jeroen van der Lubbe for their huge dedication in the support with data analyses and constructive review of the report. Javier Álvaro Blasco from Geosciences Institute-CSIC (Madrid, Spain) is shown gratitude for providing the speleothem material. Employees at ICTJA-CSIC (Barcelona, Spain) who contributed in the XRD analyses are much appreciated. Suzanne Verdegaal-Warmerdam and Onno Postma are thanked for their assist in the gathering of data for stable isotopes and fluid inclusions. I also acknowledge the kind assistance of Roel van Elsas, who aided in the SEM imaging and EDS analyses. I am grateful to Bouke Lacet, who prepared the materials used in this study by cutting, polishing and drilling the stalagmite slab, thin sections and fluid inclusion cores. Finally, I particularly thank Sarah de Bie, who reviewed the report over and over again, helped during all measurements and contributed in the comparison of this study with the one from Scladina.

Analyses were funded by the Faculty of Earth and Life Sciences of the Vrije Universiteit (VU) in Amsterdam.

References

Álvaro, J. J., Bauluz, B., Clausen, S., Devaere, L., Imaz, A. G., Monceret, E. & Vizcaino, D. 2014. Stratigraphic review of the Cambrian-Lower Ordovician volcanosedimentary complexes from the northern Montagne Noire, France. *Stratigraphy,* 11(1)**,** pp 83-96.

Álvaro, J. J., Elicki, O., Debrenne, F. & Vizcaïno, D. 2002. Small shelly fossils from the Lower Cambrian Lastours Formation, southern Montagne Noire, France. *Geobios,* 35(4)**,** pp 397-409.

Álvaro, J. J., Liñán, E. & Vizcaïno, D. 1998a. Biostratigraphical significance of the genus Ferralsia (Lower Cambrian, Trilobita). *Geobios,* 31(4)**,** pp 499-504.

Álvaro, J. J., Monceret, E., Monceret, S., Verraes, G. & Vizcaino, D. 2010. Stratigraphic record and palaeogeographic context of the Cambrian Epoch 2 subtropical carbonate platforms and their basinal counterparts in SW Europe, West Gondwana. *Bulletin of Geosciences,* 85(4)**,** pp 573-584.

Álvaro, J. J., Rouchy, J., Bechstädt, T., Boucot, A., Boyer, F., Debrenne, F., Moreno-Eiris, E., Perejón, A. & Vennin, E. 2000. Evaporitic constraints on the southward drifting of the western Gondwana margin during Early Cambrian times. *Palaeogeography, Palaeoclimatology, Palaeoecology,* 160(1)**,** pp 105-122.

Álvaro, J. J., Vennin, E. & Vizcaïno, D. 1998b. Depositional controls on Early Cambrian microbial carbonates from the Montagne Noire, southern France. *Transactions of the Royal Society of Edinburgh: Earth Sciences,* 89(03)**,** pp 135-143.

Asrat, A., Baker, A., Leng, M., Gunn, J. & Umer, M. 2008. Environmental monitoring in the Mechara caves, Southeastern Ethiopia: implications for speleothem palaeoclimate studies. *international Journal of Speleology,* 37(3)**,** pp.

Baker, A., Asrat, A., Fairchild, I. J., Leng, M. J., Wynn, P. M., Bryant, C., Genty, D. & Umer, M. 2007. Analysis of the climate signal contained within δ 18 O and growth rate parameters in two Ethiopian stalagmites. *Geochimica et Cosmochimica Acta,* 71(12)**,** pp 2975-2988.

Baker, A., Smith, C. L., Jex, C., Fairchild, I. J., Genty, D. & Fuller, L. 2008. Annually laminated speleothems: a review. *International Journal of Speleology,* 37(3)**,** pp 4.

Bemis, B. E., Spero, H. J., Bijma, J. & Lea, D. W. 1998. Reevaluation of the oxygen isotopic composition of planktonic foraminifera: Experimental results and revised paleotemperature equations. *Paleoceanography,* 13(2)**,** pp 150-160.

Blisniuk, P. M. & Stern, L. A. 2005. Stable isotope paleoaltimetry: A critical review. *American Journal of Science,* 305(10)**,** pp 1033-1074.

Boch, R., Spötl, C. & Frisia, S. 2011. Origin and palaeoenvironmental significance of lamination in stalagmites from Katerloch Cave, Austria. *Sedimentology,* 58(2)**,** pp 508-531.

Boch, R., Spötl, C. & Kramers, J. 2009. High-resolution isotope records of early Holocene rapid climate change from two coeval stalagmites of Katerloch Cave, Austria. *Quaternary Science Reviews,* 28(23)**,** pp 2527-2538.

Caroll, J. 2015. *Beech Tree Identification: Growing Beech Trees In The Landscape* [Online]. Available: https://www.gardeningknowhow.com/ornamental/trees/beech/beech-trees-in-landscapes.htm [Accessed 17 April 2017].

Comité départemental du tourisme de l'Aude. 2012. Nature & environnement, (Carcassonne).

Craig, H. 1961. Isotopic variations in meteoric waters. *Science,* 133(3465)**,** pp 1702-1703.

Craig, H. 1965. The measurement of oxygen isotope paleotemperatures. *Stable Isotopes in Oceanographic Studies and Paleotemperature,* 161-182.

Dansgaard, W. 1964. Stable isotopes in precipitation. *Tellus,* 16(4)**,** pp 436-468.

De Bie, S. E. 2017. *Climate reconstruction of Belgium using a speleothem from the Scladina cave.* Unpublished BSc thesis, Vrije Universiteit.

Fairchild, I. J. 2013. *Cave deposits (speleothems) as archives of environmental change* [Online]. Available: http://climatica.org.uk/cave-deposits-speleothems-as-archives-of-environmental-change.

Fairchild, I. J., Borsato, A., Tooth, A. F., Frisia, S., Hawkesworth, C. J., Huang, Y., McDermott, F. & Spiro, B. 2000. Controls on trace element (Sr–Mg) compositions of carbonate cave waters: implications for speleothem climatic records. *Chemical Geology,* 166(3)**,** pp 255-269.

Fairchild, I. J. & McMillan, E. A. 2007. Speleothems as indicators of wet and dry periods. *International Journal of Speleology,* 36(2)**,** pp 2.

Fairchild, I. J., Smith, C. L., Baker, A., Fuller, L., Spötl, C., Mattey, D. & McDermott, F. 2006. Modification and preservation of environmental signals in speleothems. *Earth-Science Reviews,* 75(1)**,** pp 105-153.

Fleitmann, D. & Spötl, C. 2008. Editorial: Advances in speleothem research. *PAGES NEWS: Advances in speleothem research,* 16(3)**,** pp 2.

Frisia, S. 2015. Microstratigraphic logging of calcite fabrics in speleothems as tool for palaeoclimate studies. *International Journal of Speleology,* 44(1)**,** pp 1.

Frisia, S. & Borsato, A. 2010. Karst. *Developments in sedimentology,* 61(269-318.

Frisia, S., Borsato, A., Drysdale, R., Paul, B., Greig, A. & Cotte, M. 2012. A re-evaluation of the palaeoclimatic significance of phosphorus variability in speleothems revealed by high-resolution synchrotron micro XRF mapping. *Climate of the Past,* 8(6)**,** pp 2039-2051.

Frisia, S., Borsato, A., Fairchild, I. J., McDermott, F. & Selmo, E. M. 2002. Aragonite-calcite relationships in speleothems (Grotte de Clamouse, France): environment, fabrics, and carbonate geochemistry. *Journal of Sedimentary Research,* 72(5)**,** pp 687-699.

Frisia, S., Borsato, A., Richards, D., Miorandi, R. & Davanzo, S. 2007. Variazioni climatiche ed eventi sismici negli ultimi 4500 anni nel Trentino Meridionale da una stalagmite della Cogola Grande di Giazzera implicazioni per gli studi climatico-ambientali da speleotemi, Studi Trentini di Scienze Naturali. *Acta Geol,* 82(205-223.

Fuller, L., Baker, A., Fairchild, I., Spötl, C., Marca-Bell, A., Rowe, P. & Dennis, P. 2008. Isotope hydrology of dripwaters in a Scottish cave and implications for stalagmite palaeoclimate research. *Hydrology and Earth System Sciences Discussions,* 5(2)**,** pp 547-577.

Genty, D., Blamart, D., Ouahdi, R., Gilmour, M., Baker, A., Jouzel, J. & Van-Exter, S. 2003. Precise dating of Dansgaard–Oeschger climate oscillations in western Europe from stalagmite data. *Nature,* 421(6925)**,** pp 833-837.

Genty, D., Combourieu-Nebout, N., Peyron, O., Blamart, D., Wainer, K., Mansuri, F., Ghaleb, B., Isabello, L., Dormoy, I. & von Grafenstein, U. 2010. Isotopic characterization of rapid climatic events during OIS3 and OIS4 in Villars Cave stalagmites (SW-France) and correlation with Atlantic and Mediterranean pollen records. *Quaternary Science Reviews,* 29(19)**,** pp 2799-2820.

Google Maps. 2017a. *France* [Online]. Available: https://www.google.com/maps/@45.8747894,3.3540941,6z?hl=en [Accessed 12 April 2017].

Google Maps. 2017b. *Montagne Noire* [Online]. Available: https://www.google.com/maps/@43.6543512,2.784825,120151m/data=!3m1!1e3?hl=en [Accessed 12 April 2017].

Google Maps. 2017c. *Topography Mélagues* [Online]. Available: https://www.google.nl/maps/place/43%C2%B044'33.0%22N+3%C2%B000'50.3%22E/@43.7433241,3.0088959,15.83z/data=!4m5!3m4!1s0x0:0x0!8m2!3d43.7425!4d3.0139722!5m1!1e4?hl=en [Accessed 14 April 2017].

Henderson, G. M. 2006. CLIMATE: Caving in to new chronologies. *Science,* 313(5787)**,** pp 620-622.

Hendy, C. H. 1971. The isotopic geochemistry of speleothems. 1. The calculation of the effects of different modes of formation on the isotopic composition of speleothems and their applicability as palaeoclimatic indicators. *Geochimica et cosmochimica Acta,* 35(8)**,** pp 801-824.

IAEA/WMO. 2013. *Water Isotope System for Data Analysis, Visualization, and Electronic Retrieval - Global Network of Isotopes in Precipitation* [Online]. Available: https://nucleus.iaea.org/wiser/gnip.php?ll_latlon=42.56926437219384,0.48339843749999994&ur_latlon=44.941473354802504,6.921386718749999&action=Search# [Accessed 4 June 2017].

Inventaire Forestier National. 1989. Département de l'Aude: résultats du troisième inventaire forestier, National, I. F.

Inventaire Forestier National. 1995. Département de l'Aveyron: résultats du troisième inventaire forestier, National, I. F.

Jalut, G., Amat, A. E., Bonnet, L., Gauquelin, T. & Fontugne, M. 2000. Holocene climatic changes in the Western Mediterranean, from south-east France to south-east Spain. *Palaeogeography, Palaeoclimatology, Palaeoecology,* 160(3)**,** pp 255-290.

Johnston, V., Borsato, A., Spötl, C., Frisia, S. & Miorandi, R. 2013. Stable isotopes in caves over altitudinal gradients: fractionation behaviour and inferences for speleothem sensitivity to climate change. *Climate of the Past,* 9(1)**,** pp 99.

Kaufmann, G. & Dreybrodt, W. 2004. Stalagmite growth and palaeo-climate: an inverse approach. *Earth and Planetary Science Letters,* 224(3)**,** pp 529-545.

Kendall, A. C. & Broughton, P. L. 1978. Origin of fabrics in speleothems composed of columnar calcite crystals. *Journal of Sedimentary Research,* 48(2)**,** pp.

Kim, S.-T. & O'Neil, J. R. 1997. Equilibrium and nonequilibrium oxygen isotope effects in synthetic carbonates. *Geochimica et Cosmochimica Acta,* 61(16)**,** pp 3461-3475.

Lachniet, M. S. 2009. Climatic and environmental controls on speleothem oxygen-isotope values. *Quaternary Science Reviews,* 28(5)**,** pp 412-432.

Lauritzen, S.-E. & Lundberg, J. 1999. Calibration of the speleothem delta function: an absolute temperature record for the Holocene in northern Norway. *The Holocene,* 9(6)**,** pp 659-669.

LeGrande, A. N. & Schmidt, G. A. 2006. Global gridded data set of the oxygen isotopic composition in seawater. *Geophysical research letters,* 33(12)**,** pp.

Luetscher, M., Hoffmann, D., Frisia, S. & Spötl, C. 2011. Holocene glacier history from alpine speleothems, Milchbach cave, Switzerland. *Earth and Planetary Science Letters,* 302(1)**,** pp 95-106.

McDermott, F. 2004. Palaeo-climate reconstruction from stable isotope variations in speleothems: a review. *Quaternary Science Reviews,* 23(7)**,** pp 901-918.

McDermott, F., Atkinson, T., Fairchild, I. J., Baldini, L. M. & Mattey, D. P. 2011. A first evaluation of the spatial gradients in δ18O recorded by European Holocene speleothems. *Global and Planetary Change,* 79(3)**,** pp 275-287.

McDermott, F., Frisia, S., Huang, Y., Longinelli, A., Spiro, B., Heaton, T. H., Hawkesworth, C. J., Borsato, A., Keppens, E. & Fairchild, I. J. 1999. Holocene climate variability in Europe: evidence from δ18O, textural and extension-rate variations in three speleothems. *Quaternary Science Reviews,* 18(8-9)**,** pp 1021-1038.

McDermott, F., Schwarcz, H. & Rowe, P. J. 2006. *Isotopes in speleothems*: Dordrecht, The Netherlands: Springer.

McMillan, E. A., Fairchild, I. J., Frisia, S., Borsato, A. & McDermott, F. 2005. Annual trace element cycles in calcite–aragonite speleothems: evidence of drought in the western Mediterranean 1200–1100 yr BP. *Journal of Quaternary Science,* 20(5)**,** pp 423-433.

Miorandi, R., Borsato, A., Frisia, S. & Zandonati, M. 2007. Monitoraggio di aria e acqua di percolazione in alcune grotte del Trentino. *Studi Trent. Sci. Nat., Acta Geol,* 82(2005)**,** pp 151-164.

Orland, I. J., Burstyn, Y., Bar-Matthews, M., Kozdon, R., Ayalon, A., Matthews, A. & Valley, J. W. 2014. Seasonal climate signals (1990–2008) in a modern Soreq Cave stalagmite as revealed by high-resolution geochemical analysis. *Chemical Geology,* 363(322-333.

Oster, J. L., Montañez, I. P. & Kelley, N. P. 2012. Response of a modern cave system to large seasonal precipitation variability. *Geochimica et Cosmochimica Acta,* 91(92-108.

Partin, J. W., Cobb, K. & Banner, J. L. 2008. Climate variability recorded in tropical and sub-tropical speleothems. *PAGES NEWS: Advances in speleothem research,* 16(3)**,** pp 9-10.

Perrin, C., Prestimonaco, L., Servelle, G., Tilhac, R., Maury, M. & Cabrol, P. 2014. Aragonite–calcite speleothems: identifying original and diagenetic features. *Journal of Sedimentary Research,* 84(4)**,** pp 245-269.

Plagnes, V., Causse, C., Genty, D., Paterne, M. & Blamart, D. 2002. A discontinuous climatic record from 187 to 74 ka from a speleothem of the Clamouse Cave (south of France). *Earth and Planetary Science Letters,* 201(1)**,** pp 87-103.

Riechelmann, D. 2010. Aktuospeläologische Untersuchungen in der Bunkerhöhle des Iserlohner Massenkalks (NRW/Deutschland): Signifikanz für kontinentale Klimaarchive. *PhD, Ruhr-Universität Bochum, Germany*.

Riechelmann, D. F. C., Schröder-Ritzrau, A., Scholz, D., Fohlmeister, J., Spötl, C., Richter, D. K. & Mangini, A. 2011. Monitoring Bunker Cave (NW Germany): A prerequisite to interpret geochemical proxy data of speleothems from this site. *Journal of Hydrology,* 409(3)**,** pp 682-695.

Salomon, J.-N. & Bou, C. 2012. Morphologies insolites de la Grotte des Perles (Massif Central Français). *Scientific Annals of "Alexandru Ioan Cuza" University of Iasi - Geography series: Brief communications,* 58(2)**,** pp 207-222.

Schwarcz, H. 2007. Speleothems. *Encyclopedia of Quaternary Science,* 290-300.

Stoll, H. M., Moreno, A., Mendez-Vicente, A., Gonzalez-Lemos, S., Jimenez-Sanchez, M., Dominguez-Cuesta, M. J., Edwards, R. L., Cheng, H. & Wang, X. 2013. Paleoclimate and growth rates of speleothems in the northwestern Iberian Peninsula over the last two glacial cycles. *Quaternary Research,* 80(2)**,** pp 284-290.

Sundqvist, H. S., Seibert, J. & Holmgren, K. 2007. Understanding conditions behind speleothem formation in Korallgrottan, northwestern Sweden. *Journal of hydrology,* 347(1)**,** pp 13-22.

The World Bank Group. n.d. *Country Historical Climate - France* [Online]. Available: http://sdwebx.worldbank.org/climateportal/index.cfm?page=country_historical_climate&ThisCCode=FRA [Accessed 13 May 2017].

Van Baal, R., Postma, O., Uunk, B. & Van der Lubbe, J. 2017. Stable Isotope Crusher System Version 2.0. Unpublished manuscript, Vrije Universiteit, Amsterdam.

Van Breukelen, M. 2009. *Peruvian stalagmites as archives of Holocene temperature and rainfall variability.* PhD thesis, Vrije Universiteit.

Van Breukelen, M., Vonhof, H., Hellstrom, J., Wester, W. & Kroon, D. 2008. Fossil dripwater in stalagmites reveals Holocene temperature and rainfall variation in Amazonia. *Earth and Planetary Science Letters,* 275(1)**,** pp 54-60.

Van Nunen, A. P. 2011. *Speleothem-based climate reconstruction of the Scladina cave (Belgium).* Unpublished MSc thesis, Vrije Universiteit.

Van Rampelbergh, M., Verheyden, S., Allan, M., Quinif, Y., Cheng, H., Edwards, L., Keppens, E. & Claeys, P. 2015. A 500-year seasonally resolved d18O and d13C, layer thickness and calcite aspect record from a speleothem deposited in the Han-sur-Lesse cave, Belgium. *Climate of the Past,* 11(6)**,** pp 789.

Verheyden, S. 2001. *Speleothems as palaeoclimatic archives, Isotopic and geochemical study of the cave environment and its Late Quaternary records.* Unpublished PhD Thesis, Vrije Universiteit Brussel, Belgium, 132 p.

Verheyden, S., Quinif, Y., Keppens, E., Cheng, H. J. & Edwards, L. R. 2014. Late-glacial and Holocene climate reconstruction as inferred from a stalagmite-grotte du Père Noël, Han-sur-Lesse, Belgium. *Geologica Belgica*.

Vonhof, H., Atkinson, T., Van Breukelen, M. & Postma, O. Fluid inclusion hydrogen and oxygen isotope analyses using the “Amsterdam Device”: a progress report. Geophys. Res. Abstr, 2007. 05702.

Vonhof, H., Van Breukelen, M., Postma, O., Rowe, P., Atkinson, T. & Kroon, D. 2006. A continuous-flow crushing device for on-line δ2H analysis of fluid inclusion water in speleothems. *Rapid communications in mass spectrometry,* 20(17)**,** pp 2553-2558.

Wackerbarth, A., Langebroek, P., Werner, M., Lohmann, G., Riechelmann, S., Borsato, A. & Mangini, A. 2012. Simulated oxygen isotopes in cave drip water and speleothem calcite in European caves. *Climate of the Past,* 8(6)**,** pp 1781.

Wigley, T. & Brown, M. 1976. The physics of caves. *The Science of Speleology. Academic Press, London,* 329-358.

Young, R. A. 1993. *The Rietveld method*: International Union of Crystallography.

See separate document for Appendix I-VI.